Effects of curing on the hydro-mechanical behaviour of cement-bentonite mixtures for cut-off walls

Flessati, Luca; Vecchia, Gabriele Della; Musso, Guido

DOI
10.1016/j.conbuildmat.2023.131392

Publication date
2023

Document Version
Final published version

Published in
Construction and Building Materials

Citation (APA)
Flessati, L., Vecchia, G. D., & Musso, G. (2023). Effects of curing on the hydro-mechanical behaviour of cement-bentonite mixtures for cut-off walls. *Construction and Building Materials*, *383*, Article 131392. https://doi.org/10.1016/j.conbuildmat.2023.131392

Construction and Building Materials 383 (2023) 131392

Contents lists available at ScienceDirect

Construction and Building Materials

journal homepage: www.elsevier.com/locate/conbuildmat

Effects of curing on the hydro-mechanical behaviour of cement-bentonite mixtures for cut-off walls

Luca Flessati [a,*], Gabriele Della Vecchia [b], Guido Musso [c]

[a] Faculty of Civil Engineering and Geoscience, Delft University of Technology, Delft, the Netherlands
[b] Department of Civil and Environmental Engineering, Politecnico di Milano, Milano, Italy
[c] Department of Structural, Geotechnical and Building Engineering, Politecnico di Torino, Torino, Italy

ARTICLE INFO

Keywords:
Cement-bentonite mixtures
Curing
Hydraulic conductivity
Hydro-mechanical properties
Constitutive modelling

ABSTRACT

Cement-bentonite cut-off walls are commonly employed in geoenvironmental applications to limit ground water flow and pollutant transport. The wide diffusion of this artificial material in the current practice is not only due to its low permeability, but also to its simplicity of use. In this paper, experimental evidences about the role of curing on the hydro-mechanical behaviour of cement-bentonite mixtures are presented. Different curing times and curing conditions (representative for either water saturated or hydrocarbon polluted soils) have been considered, and their effects on both hydraulic conductivity and mechanical response in oedometer and triaxial conditions have been assessed. A unified hydro-mechanical framework, accounting for the changes of material fabric occurring with curing time and environment, is formulated. The hydraulic conductivity is very well predicted by a Kozeny-Carman like equation, whereas the mechanical behaviour is finely reproduced via an enhanced elastic–plastic constitutive model.

1. Introduction

In geoenvironmental engineering applications, cutoff walls are often employed for seepage control and to limit the diffusion of pollutants [1–10]. Cement-bentonite mixtures are mainly used due to their low hydraulic conductivity, that should be lower than 10^{-8} m/s. This value, considered suitable for seepage control [11], can be further decreased by replacing part of the cement with furnace slag or fuel ash [2,3,6–8]. In addition to low hydraulic conductivity, a shear strength roughly equivalent to the surrounding soils is also required, together with a sufficient ductility to deform without the development of cracks. Unfortunately, cement-bentonite mixtures are characterized in some circumstances by a brittle mechanical response [12]. This may be critical for the barrier performance: softening, potentially inducing the development of localized failures and the formation preferential paths for the water flow, may compromise the functionality of the cut-off wall.

Due to the cement hydration process (curing), the hydraulic and mechanical behaviour of cement-bentonite mixtures change with time. In the past, this aspect has been studied from the experimental point of view [1,4,6–8,11], but most of the studies focused on analysing mixtures in which part of the cement was replaced with either furnace slag or fuel ash [2,3,6–8]. These results highlighted that, in general, both strength and stiffness increase with curing time, while permeability decreases. Deschenes et al. [1] studied the hydro-mechanical behaviour of cement bentonite mixtures, observing that both hydraulic and mechanical responses are affected by water content (or equivalently by void ratio). The authors performed tests at different curing times (up to 90 days) and observed that material strength increases with cement content and significantly increases with curing time. In contrast, permeability slightly decreases or remains constant with curing time. The hydro-mechanical behaviour of cement-bentonite mixtures was also investigated in [4]: different curing times were considered (up to 90 days) and, also in this case, both an increase in material strength and stiffness and a reduction in permeability with curing time were observed. Carreto et al. [11] addressed the hydro-mechanical response of cement-bentonite mixtures with respect to isotropic compression, highlighting that, after curing, cement-bentonite mixtures present a yield stress that increases with cement content and curing time. Moreover, in this study the authors highlighted that for low confining pressure (i.e. lower than the yield stress) the material strength and stiffness increase with curing time but, despite that hydraulic conductivity only slightly changes. Finally, Flessati et al [12] exploited the experimental mechanical response of cement-bentonite mixtures to develop a stress–strain constitutive relationship suitable for engineering applications.

* Corresponding author at: Faculty of Civil Engineering and Geoscience, Delft University of Technology, Stevinweg 1, Delft, The Netherlands.
E-mail address: l.flessati@tudelft.nl (L. Flessati).

https://doi.org/10.1016/j.conbuildmat.2023.131392
Received 10 January 2023; Received in revised form 6 April 2023; Accepted 10 April 2023
Available online 19 April 2023

Table 1
Cement-bentonite mixture composition.

Mixture	Mass ratio at preparation	
	Water/bentonite [–]	Cement/bentonite [–]
CB4	18/1	4/1
CB5	18/1	5/1
CB6	18/1	6/1

Table 2
Summary of the experimental tests, * CB5 after curing in oil not available, ** only CB5 and CB6.

	Curing time [days]				
	28	60	120	240	360
Oedometer	✓	✓	✓	✓	✓
TXCU	✓	×	×	×	✓
TXUU	✓	✓*	✓	✓**	✓
Permeameter	✓	✓	✓	✓	✓

In addition to time, cement-bentonite mixtures are also influenced by the environmental conditions during curing. For instance, having in mind the typical case of barriers for landfill confinement, in [13,14] the hydraulic behaviour of cement-bentonite mixtures cured in acid sulphate solutions is studied. The experimental permeameter test results put in evidence that hydraulic conductivity evolution during curing is not monotonic: it initially decreases and it subsequently increases. According to the authors this is due to a clogging due to the deposition of calcium carbonate and to the advance of the reaction front. Analogously, [15] also the mechanical properties of cement-bentonite mixtures are shown to be affected by the presence of sulphates in curing water. In particular, the experimental tests shown that during curing uniaxial strength initially increases and subsequently it decreases.

The aim of this paper is to evaluate, by interpreting experimental laboratory test results, the impact of curing time and environment on the hydro-mechanical response of cement-bentonite mixtures. Specimens with different cement/bentonite ratios were prepared in the laboratory and experimental tests were performed after different curing times, in different curing conditions. During curing, the specimens hardened and consolidated under their self-weight. Two different curing conditions were considered: the specimens, after preparation, were immersed either in water or in liquid paraffin oil, a non-toxic hydrocarbon fluid used to simulate the recurring operating conditions where cut-off walls are built to isolate polluting Non Aqueous Phase Liquids (NAPLs) from clean groundwater. This second condition leads to a null water and solute exchange between the specimen and the surrounding.

From an engineering perspective, the possibility of predicting the hydraulic properties and mechanical behaviour for different curing times is of fundamental importance for cut-off wall design, both in terms of serviceability and resistance. As the stress state in engineering works is not homogeneous, experimental results are interpreted in light of a mechanical constitutive relationship (built on basis of the one proposed by Flessati et al. [12]), that allows the mechanical response and porosity to be modelled under different stress conditions. As for hydraulic purposes, the experimental evidences are exploited to link the material porosity to the hydraulic conductivity through a modified Kozeny Carman expression, whose main parameter is set to depend on curing time and environment.

2. Experimental tests

The experimental tests, carried out in the Geotechnical Laboratory of Politecnico di Torino, were aimed at studying the influence of curing on the hydro-mechanical behaviour of cement-bentonite mixtures. The mechanical behaviour was studied by performing both oedometer and undrained triaxial tests (both consolidated and non-consolidated, hereafter named TXCU and TXUU, respectively). Hydraulic conductivity was estimated by interpreting oedometer test results.

Specimens of three different cement-bentonite mixtures (CB4, CB5 and CB6) were prepared by mixing in different proportions water, Portland cement (CEM I 32.5 N) and a sodium bentonite (specific gravity 2.95, liquid limit 535% and plastic limit 75%), as summarized in Table 1. By following the procedure employed in [10], the preparation consisted of three steps: (i) water and bentonite were mixed by using a laboratory mixer; (ii) after 24 h, during which bentonite hydration took place, cement was added and the slurry was mixed again; (iii) the mixtures were poured into cylindrical molds of height 76.2 mm and 20 mm, in order to obtain specimens ready for mechanical testing (triaxial and oedometer, respectively). In all the cases, the time between steps (ii) and (iii) was always lower than 5 min. To reduce uncertainties, all the samples relative to a given mixture were obtain by using the same slurry. The subsequent curing stage was performed by immersing the specimens into two different liquids, namely water and paraffin oil. Experimental tests were performed after different curing times (t), as summarized in Table 2.

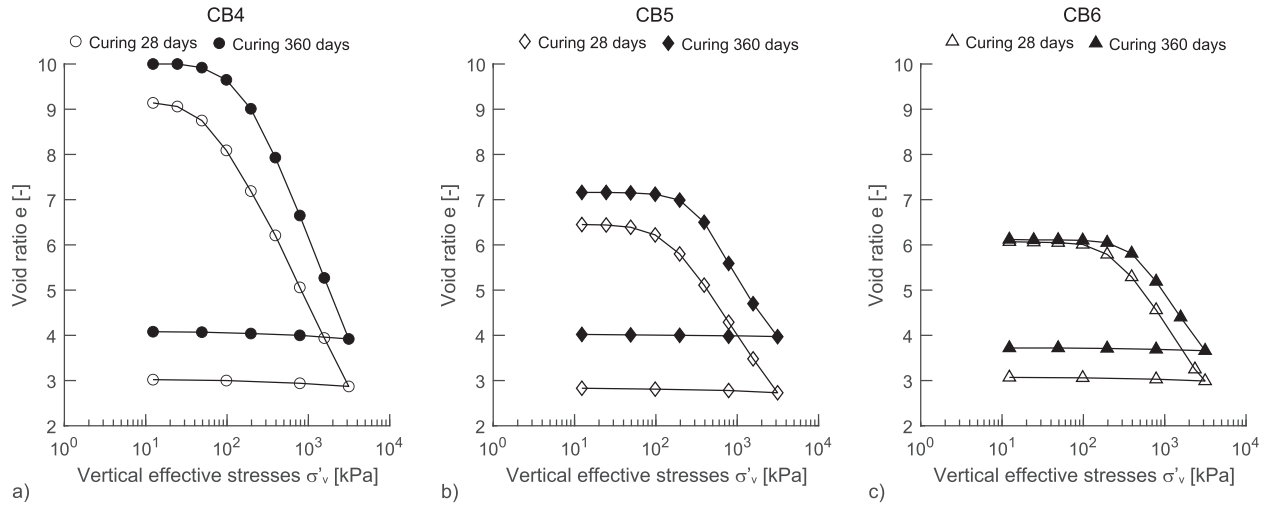

Fig. 1. Compression curves for the oedometer tests at different curing times (curing in water): a) mixture CB4, b) mixture CB5 and c) mixture CB6.

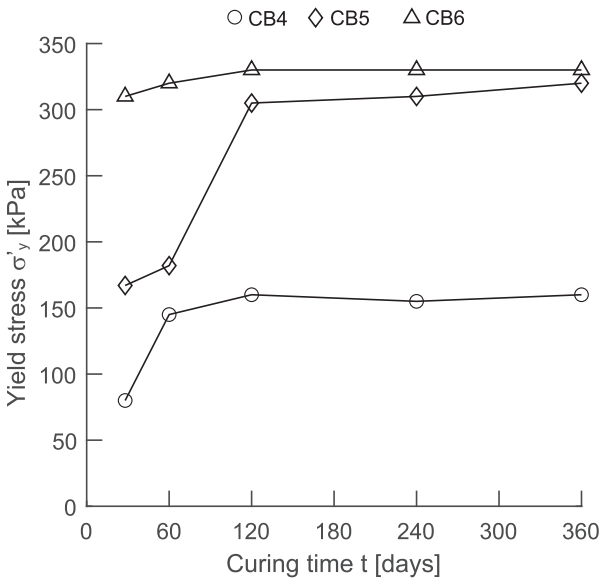

Fig. 2. Variation of yield stress with curing time (curing in water).

3. Experimental results

3.1. Curing in water

3.1.1. Mechanical behaviour

The oedometer test results relative to the three mixtures and two different curing times (28 and 360 days) are plotted in Fig. 1 in the $e-\sigma_v^{'}$ compression plane, being e and $\sigma_v^{'}$ the void ratio and the vertical effective stress, respectively. It is worth remarking that the void ratio (namely, the volume of the voids over the volume of the solids of a porous medium representative volume) is related with porosity n via the expression $n = e/(1 + e)$.

The compression curves of Fig. 1 clearly show that the initial void ratio depends on the cement/bentonite mass ratio: larger values of cement/bentonite mass ratio are associated to lower void ratios (as also observed in [11;12]), due to a "more dense" crystalline structure [11] that characterizes larger cement contents. Moreover, the experimental results also put in evidence the larger void ratio of the specimens cured for 360 days. The experimental results also evidence a steep change in stiffness at a given vertical stress, as shown when the pre-consolidation stress is reached along oedometer compression of soils. In soil mechanics, preconsolidation is recognised to be mostly related to the maximum vertical stress applied in the past and to creep. As no vertical stress was applied on the specimen top during curing the use of the term 'yield stress' instead of 'preconsolidation stress' appears to be more correct This yield stress ($\sigma_y^{'}$) was estimated by using the standard procedure introduced by Casagrande, (see e.g. [13]). It increases with both the cement/bentonite mass ratio value and curing time, as shown in Fig. 2 (where other curing times than 28 and 360 days have been also introduced) and can be related to the presence of cementation bonds between particles [11–12]. According to Fig. 2, $\sigma_y^{'}$ significantly increases for curing times up to 120 days, while it remains practically constant for larger curing times. Moreover, the experimental results also emphasise that the increment in $\sigma_y^{'}$ with curing time is more evident for lower cement/bentonite mass ratios (CB4 and CB5). Vice versa the slopes of both unloading–reloading (C_s) and the virgin loading line (C_c) slightly decrease with curing time, as also found by [8,11].

The TXCU tests were performed at different initial effective confining pressures $p_c^{'}$, for curing times of both 28 and 360 days. Experimental data for mixtures CB4 and CB6 are reported in Figs. 3 and 4, respectively. Results were plotted (i) in the $q-\varepsilon_a$ plane (where ε_a is the imposed axial strain, while q is the deviator stress) in Fig. 3a and 4a, (ii) in the $\Delta u_w-\varepsilon_a$ plane (Δu_w is the excess pore water pressure accumulated during the shearing stage of the test) in Fig. 3b and 4b and (iii) in the $q-p'$ plane (p' is the average effective pressure) in Fig. 3c and 4c.

For both curing times, when the confining pressure is significantly lower with respect to the yield stress identified in the compression curves of Fig. 1, the stress deviator monotonically increases up to an asymptotic value (Fig. 3a and 4a), while the initially increasing excess pore water pressure starts decreasing ("dilatant behaviour") at an axial strain value of approximately 1% (Fig. 3b and 4b). On the contrary, if the confining pressure is slightly smaller than the yield pressure (mixtures CB4, $p_c^{'}$=100 kPa and curing time 28 days) both q and Δu_w monotonically increase up to an asymptotic value ("contractive behaviour"). Finally, in case of confining pressure almost coincident with the yield pressure a peak and a subsequent softening branch are evident in the $q-\varepsilon_a$ plane (CB6, $p_c^{'}$=300 kPa for both curing times). During the softening branch, as is also observed in [11,16], Δu_w practically remains constant and the effective stress path in the q-p′ plane is inclined of 3.

Material strength was interpreted by using the conventional Mohr-Coulomb failure envelope. The values of friction angle (ϕ') and cohe-

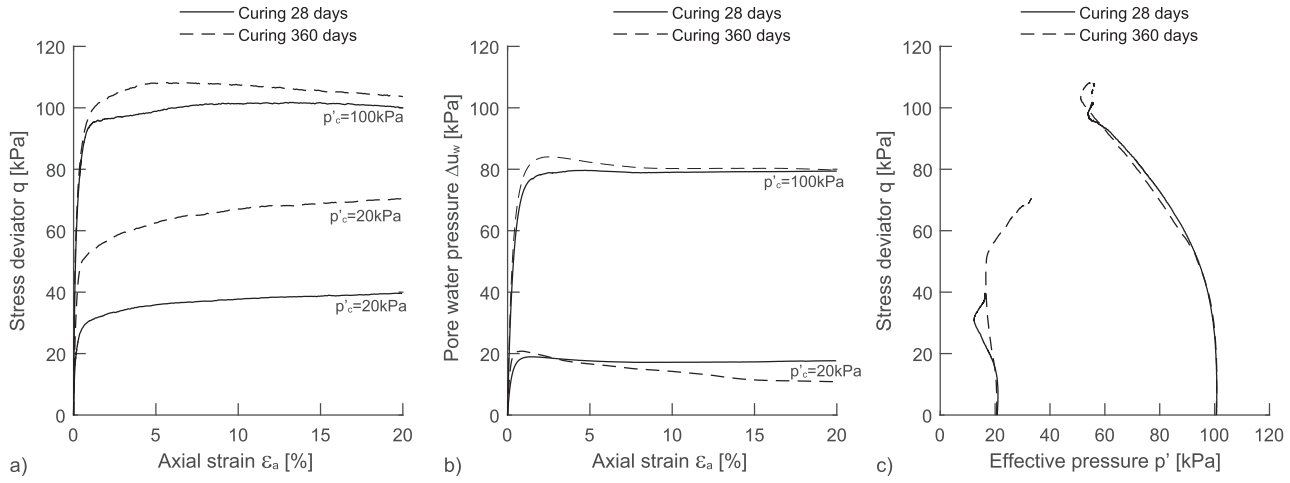

Fig. 3. Mixture CB4 triaxial tests ($p_c^{'}$ = 20 and 100 kPa) results (curing in water): a) $q-\varepsilon_a$ plane, b) $\Delta u_w-\varepsilon_a$ plane and c) $q-p'$ plane.

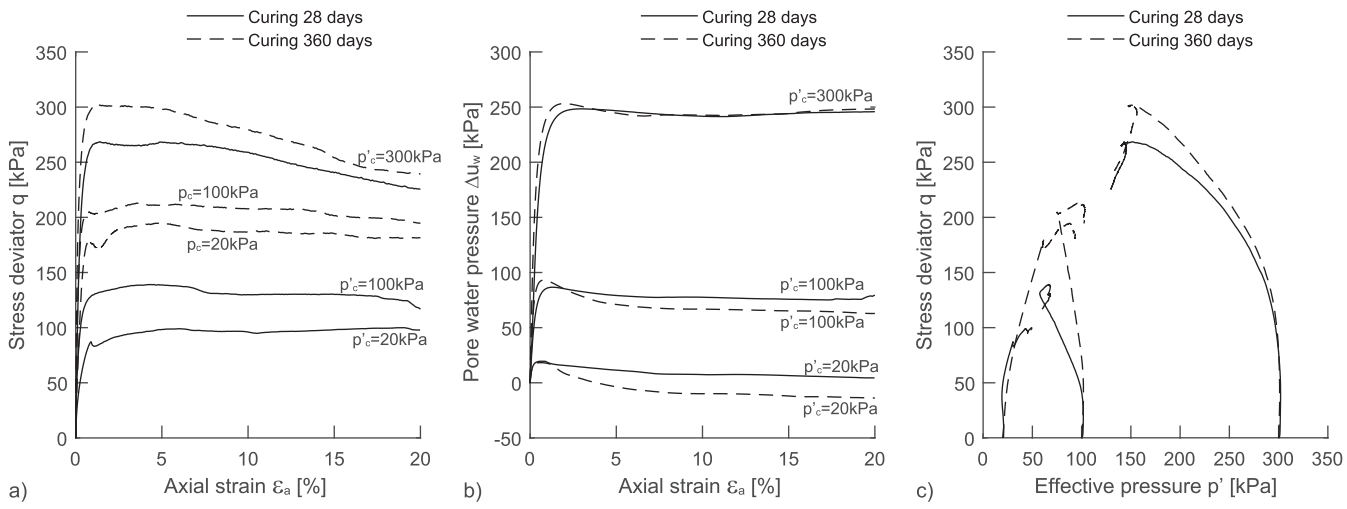

Fig. 4. Mixture CB6 triaxial tests ($p_c^{'}$ = 20, 100 and 300 kPa) results (curing in water): a) $q-\varepsilon_a$ plane, b) $\Delta u_w-\varepsilon_a$ plane and c) $q-p'$ plane.

Table 3
Mohr-Coulomb strength parameters from TXCU tests.

	CB4		CB5		CB6	
	t = 28 days	t = 360 days	t = 28 days	t = 360 days	t = 28 days	t = 360 days
c′ [kPa] (water)	4	8	11	18	17	47
ϕ′ [°] (water)	45	44	44	41	39	34
c′ [kPa] (paraffin oil)	4	20	11	38	17	36
ϕ′ [°] (paraffin oil)	45	42	44	37	39	37

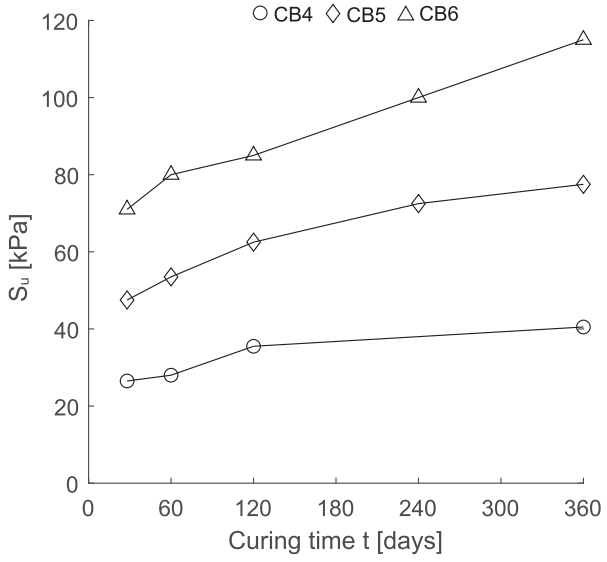

Fig. 5. TXUU tests (curing in water): variation of undrained strength with curing time.

sion (c′) obtained from the TXCU tests are summarized in Table 3. The friction angle decreases by increasing both cement/bentonite mass ratio and curing time, differently from cohesion, which increases with both cement/bentonite mass ratio and curing time.

To perform the TXUU tests a pressure of 50 kPa was imposed in the triaxial cell and the back pressure was directly measured. All the results are characterized by a continuous increase in q with ε_a (Appendix A). The values of undrained strength S_u, reported in Fig. 5, were conventionally derived as the deviator stress corresponding to an axial strain of 15%. The experimental results highlight a general trend of undrained strength increasing with curing time as was also observed in [1,4].

3.1.2. Hydraulic behaviour

The variations in hydraulic conductivity (k) with both effective vertical stresses and void ratio, relative to mixture CB4 after 28 days of curing, are reported in Fig. 6a and 6b, respectively. As is also discussed in [11], for vertical stresses lower than $\sigma_y^{'}$, the variations in k are very small, whereas for vertical stresses larger than $\sigma_y^{'}$, k significantly decreases by increasing vertical stresses. This is consistent with the mechanical response of the material, which is characterized by a larger stiffness (lower e variations) for stresses lower than $\sigma_y^{'}$ (Fig. 1). Vice-versa, when the material is 'virgin' from the mechanical point of view, i.e. the current stress is larger than the initial yield stress $\sigma_y^{'}$, the stiffness is lower and the reduction in void ratio with vertical stresses is much larger. Consistently, k variations were interpreted as dependent only on void ratio changes and modelled via a Kozeny–Carman-like equation, as already proposed for other geomaterials [17,18]:

$$k = B\frac{e^{5.5}}{1+e} \tag{1}$$

B is used here as a fitting parameter which accounts for the effects of tortuosity and specific surface (in fact, the permeability decreases as the tortuosity and the specific surface increase). In Eq. (1), the impact of the stress state on the permeability is implicitly introduced as the void ratio depends on the stress. The fitting curve obtained by imposing B = $6{\cdot}10^{-12}$ m/s is reported in Fig. 6b. By following the same procedure (the comparison between experimental results and fitting curves is reported in Appendix B), the evolution of B with curing time for the different mixtures can be derived (Fig. 7). The three curves of Fig. 7 are characterized by a progressive decrease of B with curing time, highlighting the beneficial effect of curing on the hydraulic behaviour. According to [11], the reduction in hydraulic conductivity is due to the progressive

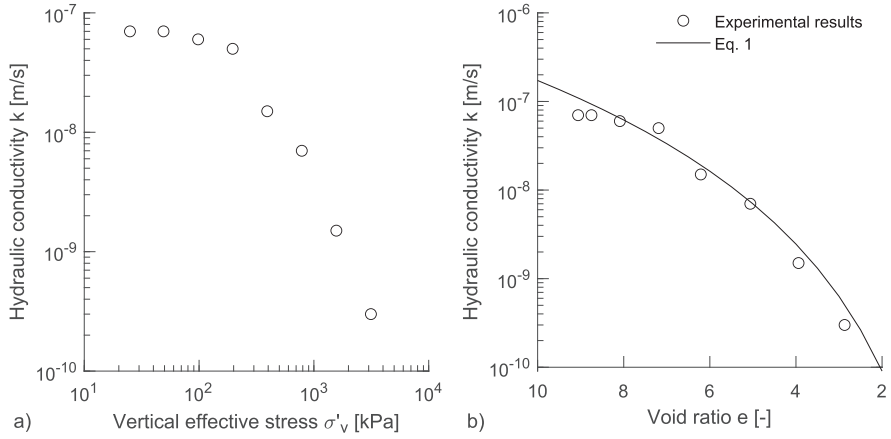

Fig. 6. Variation of hydraulic conductivity (mixture CB4, cured for 28 days in water) with a) vertical effective stresses and b) void ratio.

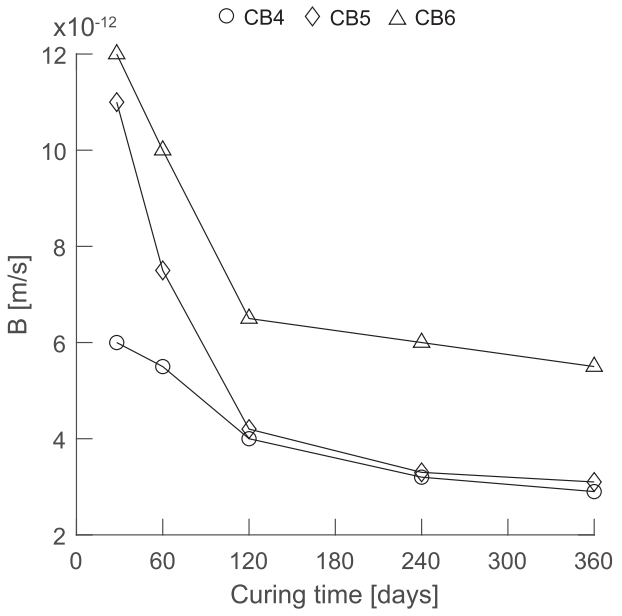

Fig. 7. Variation of Kozeny-Carman coefficient B with curing time (curing in water).

reduction in intergranular pore size due to the formation of layers of cementitious products.

3.2. Curing in paraffin oil

3.2.1. Mechanical behaviour

In Fig. 8, the oedometer test results relative to mixtures CB4 and CB6 cured in paraffin oil (t = 28 and 360 days) are compared with the ones cured in water. After 28 days of curing, a difference due to curing conditions is evident only for mixture CB4 (Fig. 8a): curing in paraffin oil is associated with a lower initial void ratio and a larger yield stress. Viceversa, both the logarithmic compliance C_c and C_s are almost coincident. For mixture CB6 (Fig. 8b), the responses of the specimens cured in water and paraffin oil are almost identical. However, by increasing curing time (Fig. 8c and d), the difference due to curing conditions becomes more pronounced. As already observed for curing in water, an increase of curing time in paraffin oil is associated to lower C_s and C_c and to a larger yield stress (Fig. 9, where the data relative to mixture CB5 and different curing times are also plotted).

Again, similarly to the water case, (i) $\sigma_y^{'}$ increases with curing time for the first 120 days, whereas it remains practically constant for larger times and (ii) the increment in $\sigma_y^{'}$ is more evident for CB4 and CB5 than CB6 (Fig. 9). By comparing the values relative to the two different curing conditions (Figs. 2 and 9), it is evident that, especially for mixture CB4, curing in paraffin oil is associated with larger $\sigma_y^{'}$ values.

In Figs. 10 and 11 the TXCU test results relative to CB4 and CB6 cured in paraffin oil are compared with the corresponding ones relative to samples cured in water. As inferred from oedometer test results, for large cement/bentonite mass ratio values (mixture CB6) the material mechanical behaviour is only slightly affected by curing conditions. For low cement/bentonite mass ratio values (mixture CB4) a significative influence is observed especially at low confining pressure: the material strength and dilatancy are larger in case of curing in paraffin oil. This agrees with the increase in yield pressure highlighted by oedometer tests.

The material strength was interpreted by using the Mohr-Coulomb failure envelope and the values of ϕ' and c' obtained from the tests are summarized in Table 3. Friction angle decreases by increasing both cement/bentonite mass ratio and curing time, while cohesion increases with both cement/bentonite mass ratio and curing time. These changes are less marked than in the case of curing in water.

The results of TXUU tests are summarized in terms of S_u in Fig. 12 (the other results are reported in Appendix A). The experimental results highlight an increase in material strength with curing time. In this case, the increment is more evident for mixtures CB5 and CB6, whereas slight variations are observed for mixture CB4.

3.2.2. Hydraulic behaviour

As for curing in water, even in this case hydraulic conductivity is affected by both mixture composition and curing time. The experimental results in terms of variation of k with e can be reproduced by using Eq. (1) (Appendix B) and the variation of B with curing time for the three mixtures is reported in Fig. 13. Also with immersion in paraffin oil curing is beneficial, as is testified by the decreasing trend of the three curves of Fig. 13. However, it is worth mentioning that B values are always larger than the ones obtained in case of curing in water (Fig. 7). This suggests that, curing in paraffin oil is beneficial in terms of mechanical behaviour, but it is not in terms of hydraulic properties.

3.2.3. Interpretation of the different response of the mixtures to the curing environment accounting for their constituents properties

Even for different curing environments, most material properties (yield stress, permeability, strength) of all the mixtures evolve with time

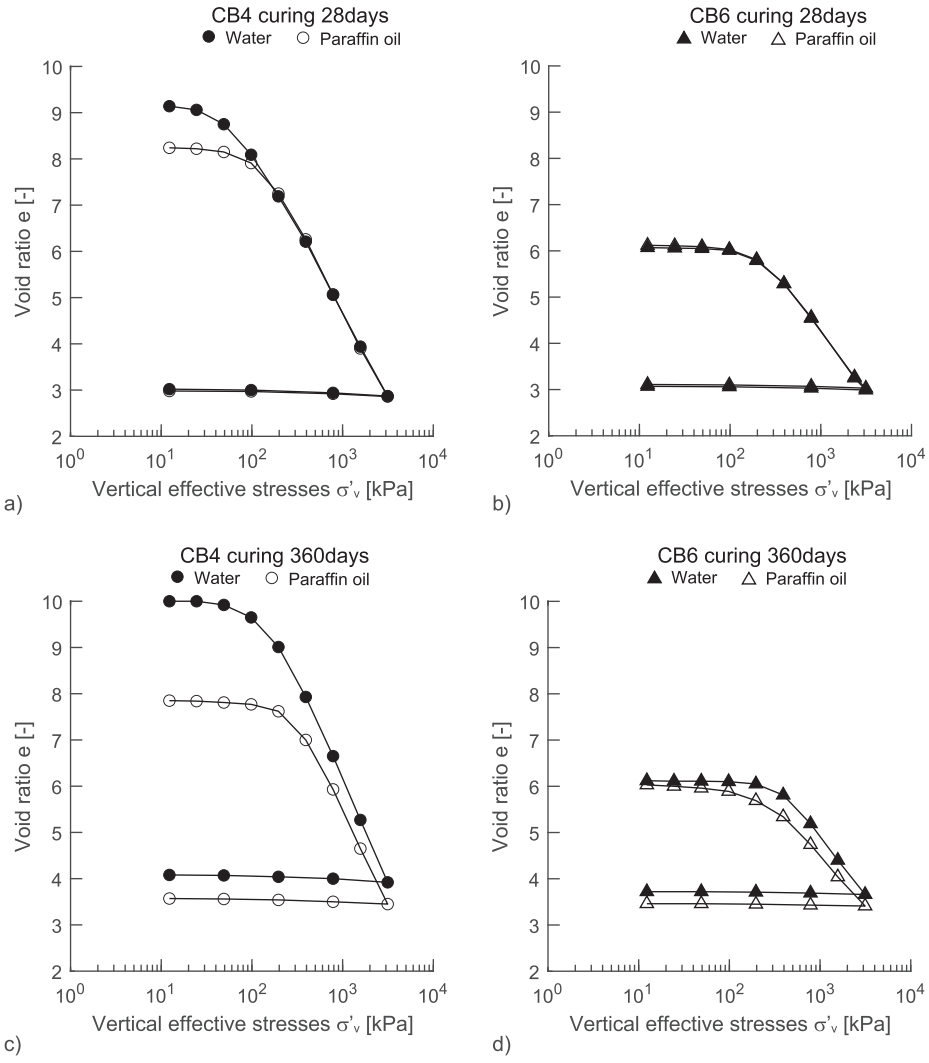

Fig. 8. Comparison between curing in water and in paraffin oil: oedometer test results: a) mixture CB4 after 28 days of curing, b) mixture CB4 after 360 days of curing, c) mixture CB6 after 28 days of curing and d) mixture CB6 after 360 days of curing.

in a similar manner. The influence of the curing environment can be appreciated by comparing, at given curing times, the behaviour of samples of the same mixture cured in different environments. Differences are larger for the samples with the highest bentonite fraction (CB6) and they are less significant for the samples with the lowest bentonite fraction (CB4). In general, it is observed that the void ratio of the samples cured in water had a certain tendency to increase with time (see results Fig. 8), not detected for the samples cured in paraffin oil. The unconfined compressive strength is generally larger with paraffin oil (Fig. 12) than with water (Fig. 5) and the same can be said regarding the yield stress (Fig. 9 and Fig. 2, respectively). Also the Kozeny-Carman parameter B, and thus the hydraulic conductivity for a given void ratio, is larger in the case of paraffin oil than in the case of water (Fig. 13 vs. Fig. 7).

While an exhaustive quantitative analysis of the physical–chemical reasons for these differences is beyond the scope of the paper, a qualitative explanation is here proposed on basis of the existing literature regarding the impact of the pore fluid chemistry on the fabric and hydro-mechanical behaviour of bentonites. Despite for all the mixtures the cement mass is predominant with respect to the bentonite one, it should be considered that in virtue of the small size of its particles, bentonite has a very large specific surface (ranging between 700 and 840 m^2/g, see e.g. [19]). Although a complex granular micro-structure is formed by the interaction between the bentonite and the products of the cement reactions (see [12,20]), its relevance is still clear recognizing that chemo-mechanical effects increase with the specific surface. The relevance of pH and pore fluid salinity in the behaviour of clays, and particularly of bentonites, is well known in geotechnical engineering (e.g. [21–23]).

Cement hydration and pozzolanic reaction cause, on the one hand, the precipitation of hydrated CSH and CAH. On the other hand, according to [20], they also causes three major changes in the pore fluid chemistry which are likely to modify the properties of the bentonite slurries: (i) a strong pH rise; (ii) a supersaturation of Ca^{2+} ions; and a non-negligible K^{+} ion concentration.

A progressive diffusion, and therefore dilution, of the reaction products from the sample pore fluid to curing bath was allowed when water was used as curing fluid. As paraffin oil is immiscible with water, diffusion cannot occur when this is used as curing fluid. While cement bonding remains the distinctive hallmark of the behaviour of the cement-bentonite mixtures, the impact of the curing environment can still be related to the impact of the pore fluid concentration on the bentonite response, as for the latter a decrease in the solute concentration was recognised to induce swelling ('osmotic swelling', see e.g. [21]), to decrease the permeability (e.g. [22–23]), to reduced shear strength (e.g. [21]) and to decrease the yield stress ([24]).

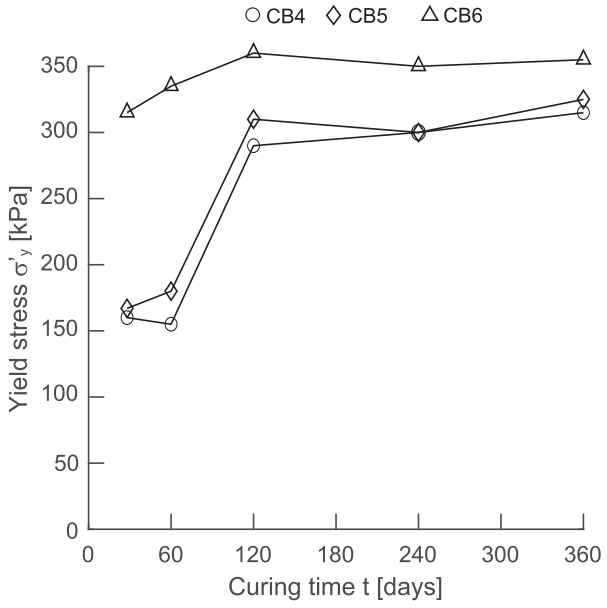

Fig. 9. Variation of yield stress with curing time (curing in paraffin oil).

4. Constitutive modelling

To reproduce the mechanical behaviour of cement-bentonite mixtures, a strain hardening elastic plastic constitutive relationship, named Cement Bentonite Constitutive (CBC) model, was introduced in [12]. This model, by following an approach similar to that suggested for compacted clayey silts in [25], was conceived by introducing in the well-known Modified Cam Clay model some features commonly employed to reproduce the undrained mechanical behaviour of granular materials [26,27]. The CBC model proved able to reproduce the mechanical behaviour of cement-bentonite mixtures, but for increasing curing time the yield stress of the material increases and a more suitable shape of the yield surface on the so-called "dry side" (i.e. for stress much lower than the yield stress) becomes relevant. A correct reproduction of the material behaviour at low confining pressures, relevant for the environmental application of cut-off walls, is in fact crucial to predict the integrity of the barrier. For this reason, to improve the constitutive model predictions, the Modified Cam Clay yield function adopted in [12] has been here substituted with the one proposed in [28]:

$$f = \frac{\left(1+\frac{q}{Mp' K_2}\right)^{\frac{K_2(K_1-K_2)}{1-m}}}{\left(1-\frac{q}{Mp' K_1}\right)^{\frac{K_1(K_1-K_2)}{1-m}}} - \frac{p'_s}{p'} \tag{2}$$

being

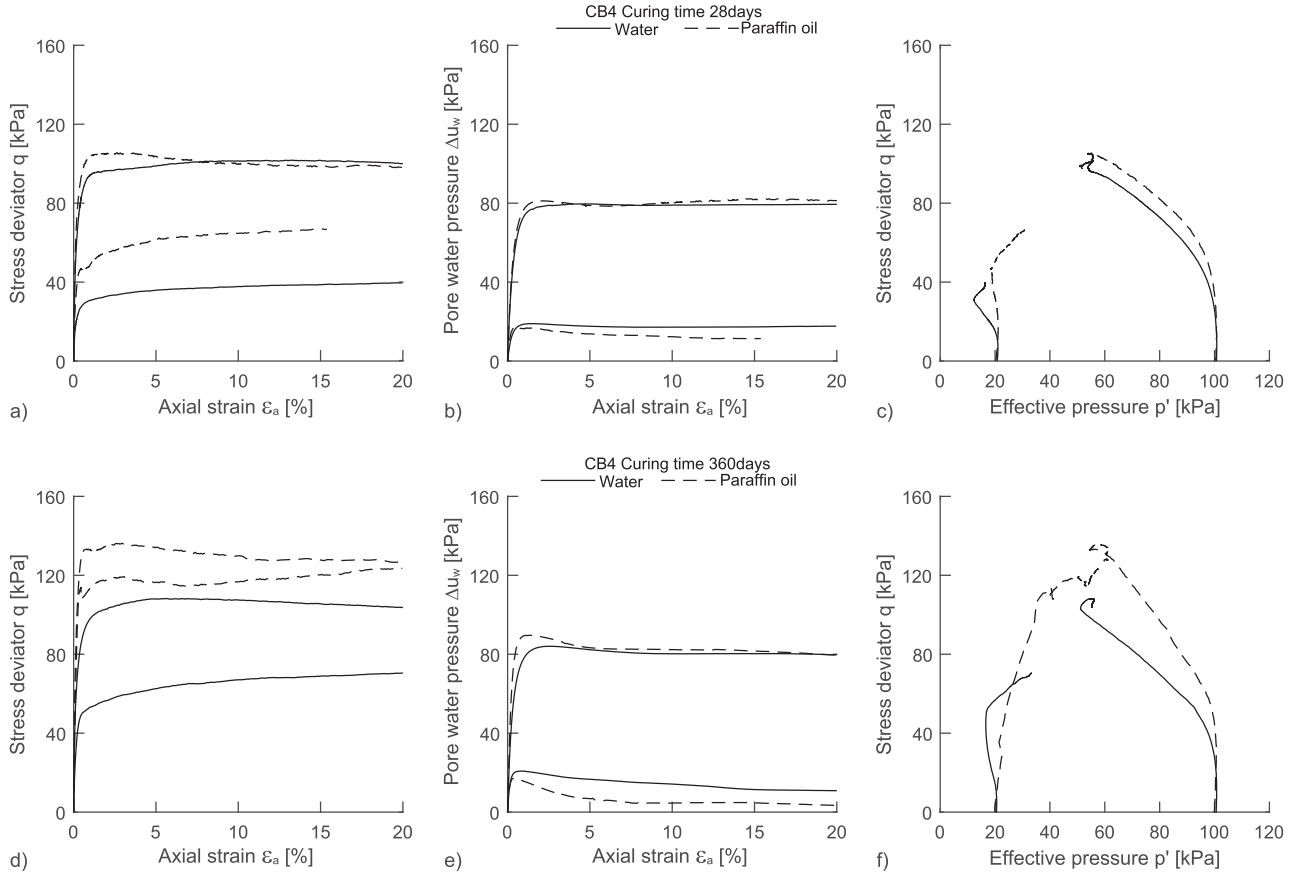

Fig. 10. Mixture CB4 triaxial tests (p'_c = 20 and 100 kPa) results: a) $q-\varepsilon_a$ plane curing 28 days, b) $\Delta u_w-\varepsilon_a$ plane curing 28 days, c) $q-p'$ plane curing 28 days, d) $q-\varepsilon_a$ plane curing 360 days, e) $\Delta u_w-\varepsilon_a$ plane curing 360 days and f) $q-p'$ plane curing 360 days.

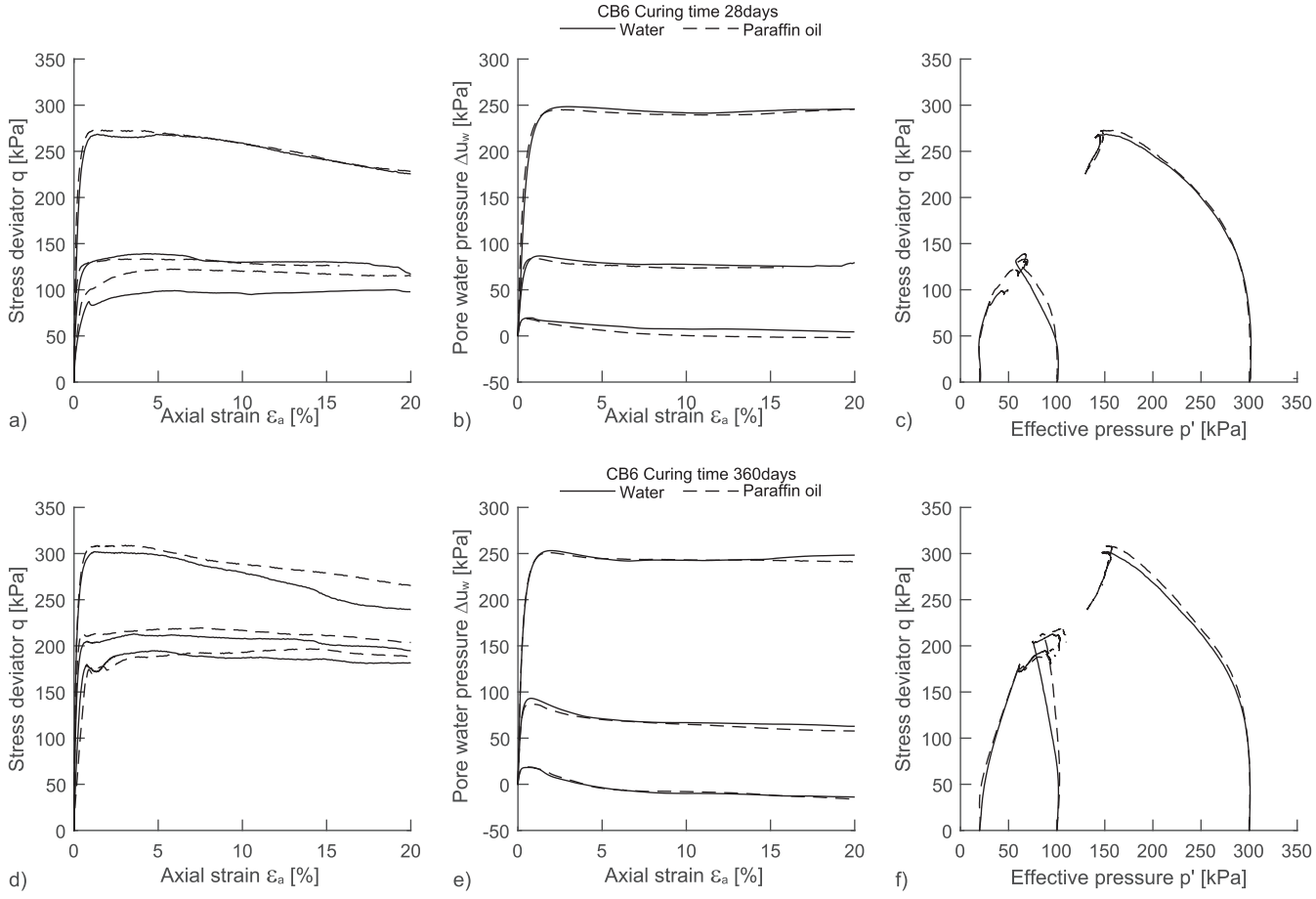

Fig. 11. Mixture CB6 triaxial tests ($p_c^{'}$ = 20, 100 and 300 kPa) results: a) $q-\varepsilon_a$ plane curing 28 days, b) $\Delta u_w-\varepsilon_a$ plane curing 28 days, c) $q-p'$ plane curing 28 days, d) $q-\varepsilon_a$ plane curing 360 days, e) $\Delta u_w-\varepsilon_a$ plane curing 360 days and f) $q-p'$ plane curing 360 day.

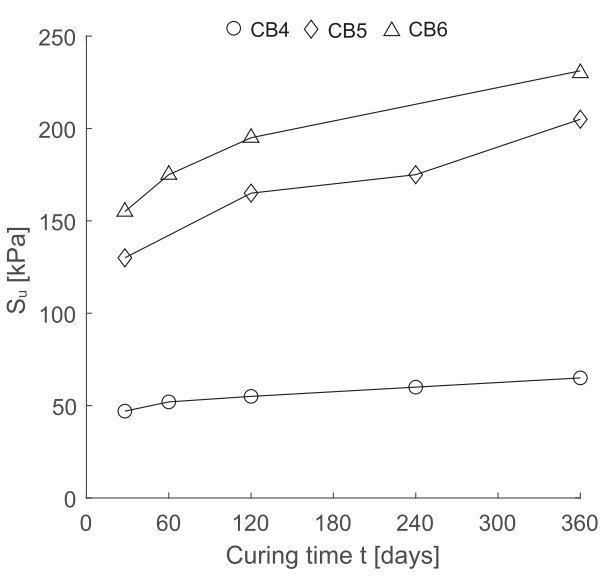

Fig. 12. Summary of the TXUU tests: variation of S_u with curing time (curing in paraffin oil).

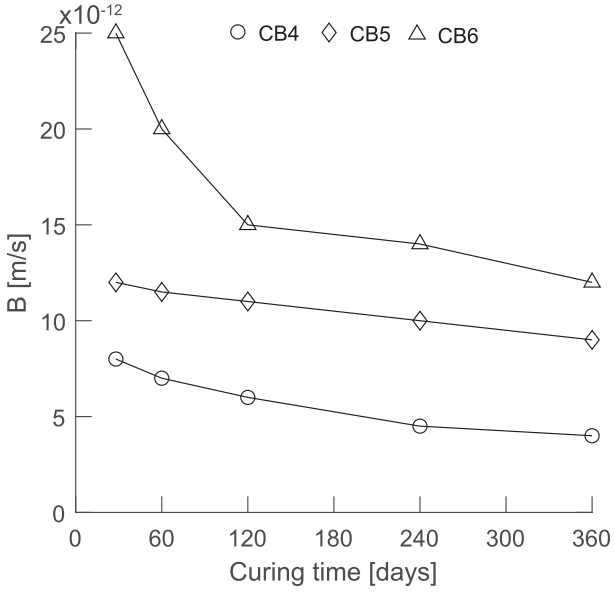

Fig. 13. Variation of Kozeny-Carman coefficient B with curing time (curing in paraffin oil).

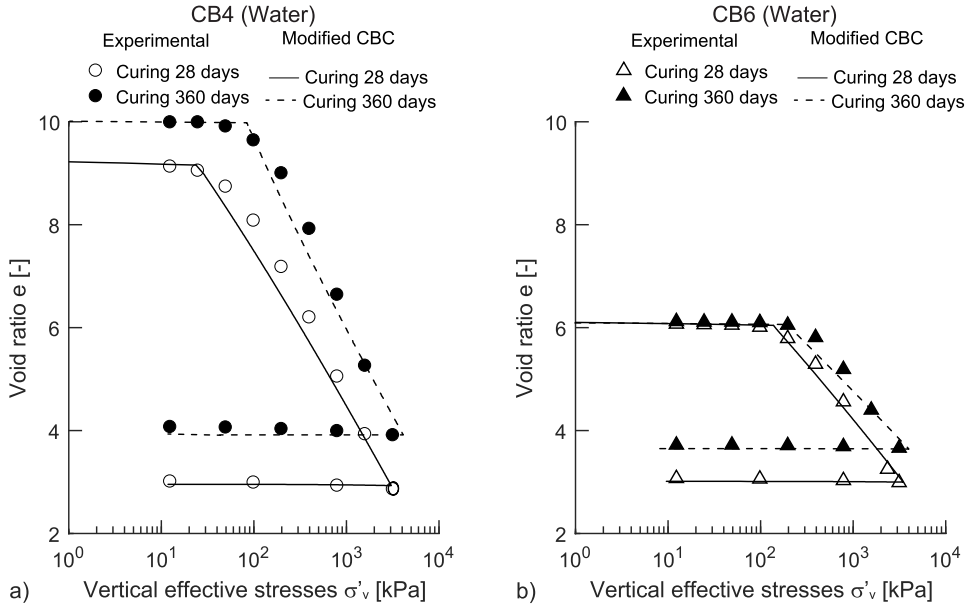

Fig. 14. Comparison between experimental results and model predictions: oedometer tests (curing in water).

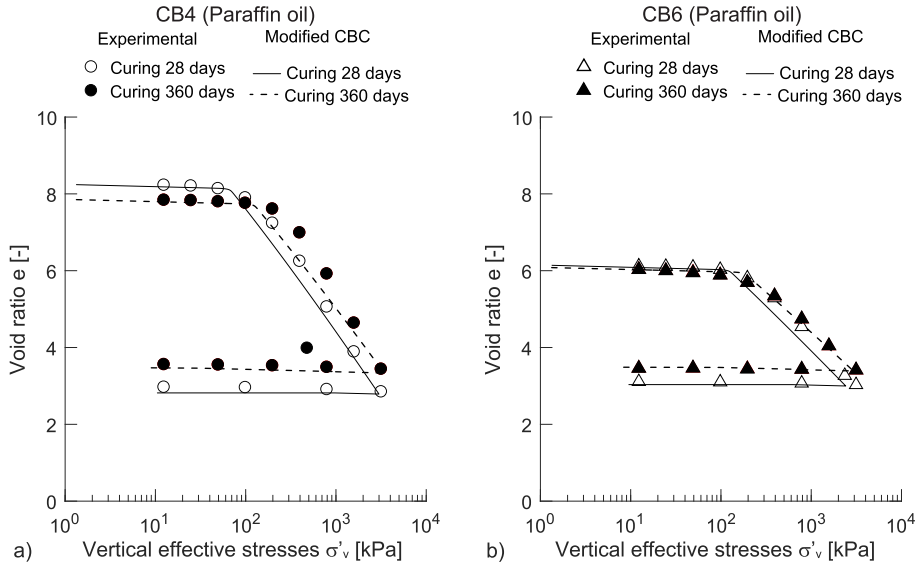

Fig. 15. Comparison between experimental results and model predictions: oedometer tests (curing in paraffin oil).

$$K_{1,2} = \frac{m(1-a)}{2(1-m)}\left\{1 \pm \left[1 - \frac{4a(1-m)}{m(1-a)^2}\right]^{1/2}\right\}, \tag{3}$$

where M is the slope of the critical state line in the $q - p'$ plane, $p_s^{'}$ the hardening variable, m and a non-dimensional constitutive parameters governing the shape of the yield function.

The direction of the plastic strain increment can be calculated according to the flow rule proposed in [27]:

$$d = M\exp(g_1\psi) - \frac{q}{p^{'}} \tag{4}$$

being d the dilatancy (i.e. the ratio between the volumetric and the deviatoric plastic strain increments), g_1 a non-dimensional constitutive parameter and ψ the state variable as defined in [26], i.e. the difference between the current void ratio and the void ratio on the critical state line at the same confining pressure. In the $e - \ln p'$ plane the critical state line is assumed to be a straight line defined by two parameters λ and Γ, the former one defining the line inclination, the latter one the critical void ratio for $p' = 1$ kPa.

The hardening rule, which links the hardening variable evolution to the plastic strain increment is here expressed in terms of hardening modulus H:

$$H = \left(p_s^{'}\frac{1+e_0}{\lambda-\kappa}\right)h_1\left[\frac{Mp^{'}}{q} - \exp(h_2\psi)\right] \tag{5}$$

where e_0 is the initial value of e, κ the slope of the unloading–reloading line in the $e - \ln p'$ (and thus mathematically related to C_s), whereas h_1 and h_2 are two non-dimensional constitutive parameters.

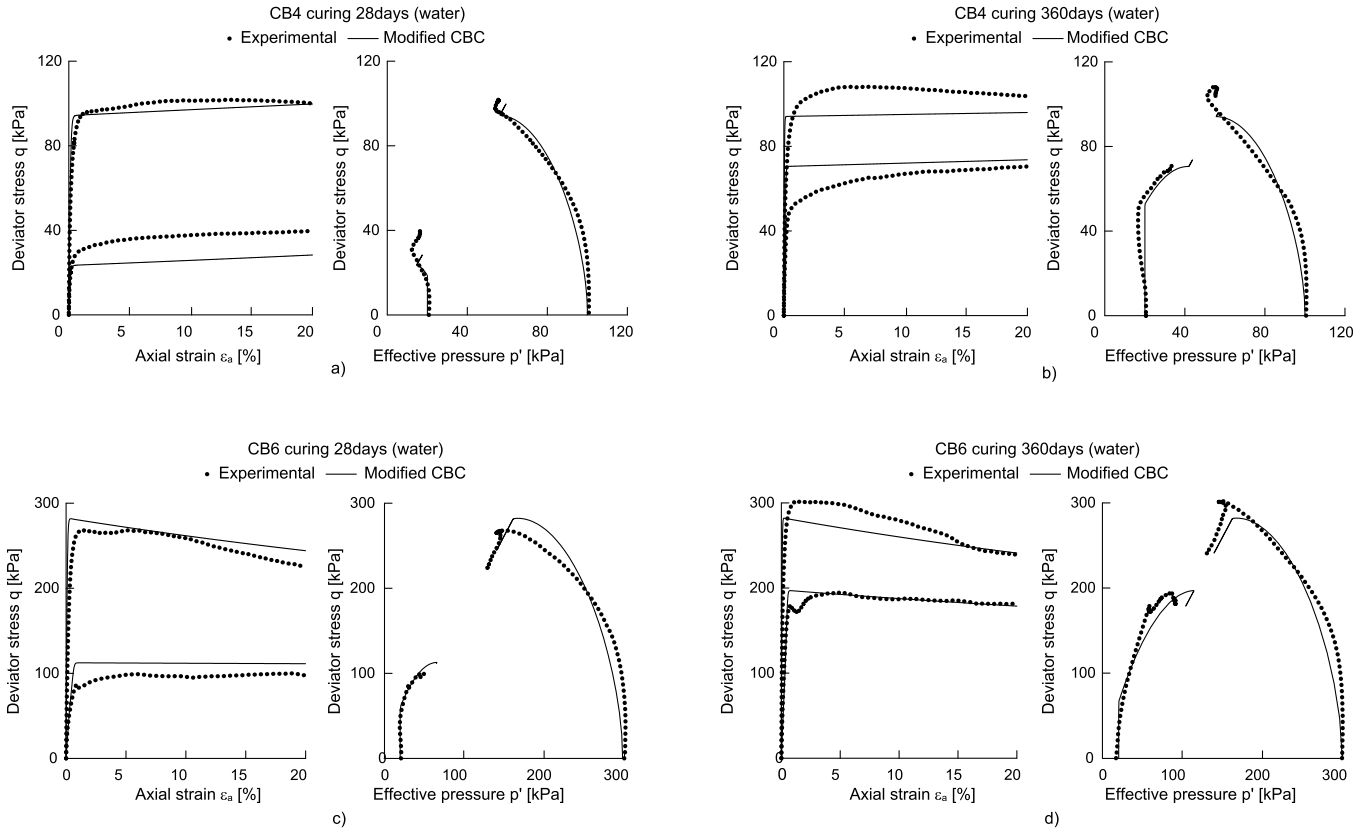

Fig. 16. Comparison between experimental results and model predictions: triaxial tests (curing in water).

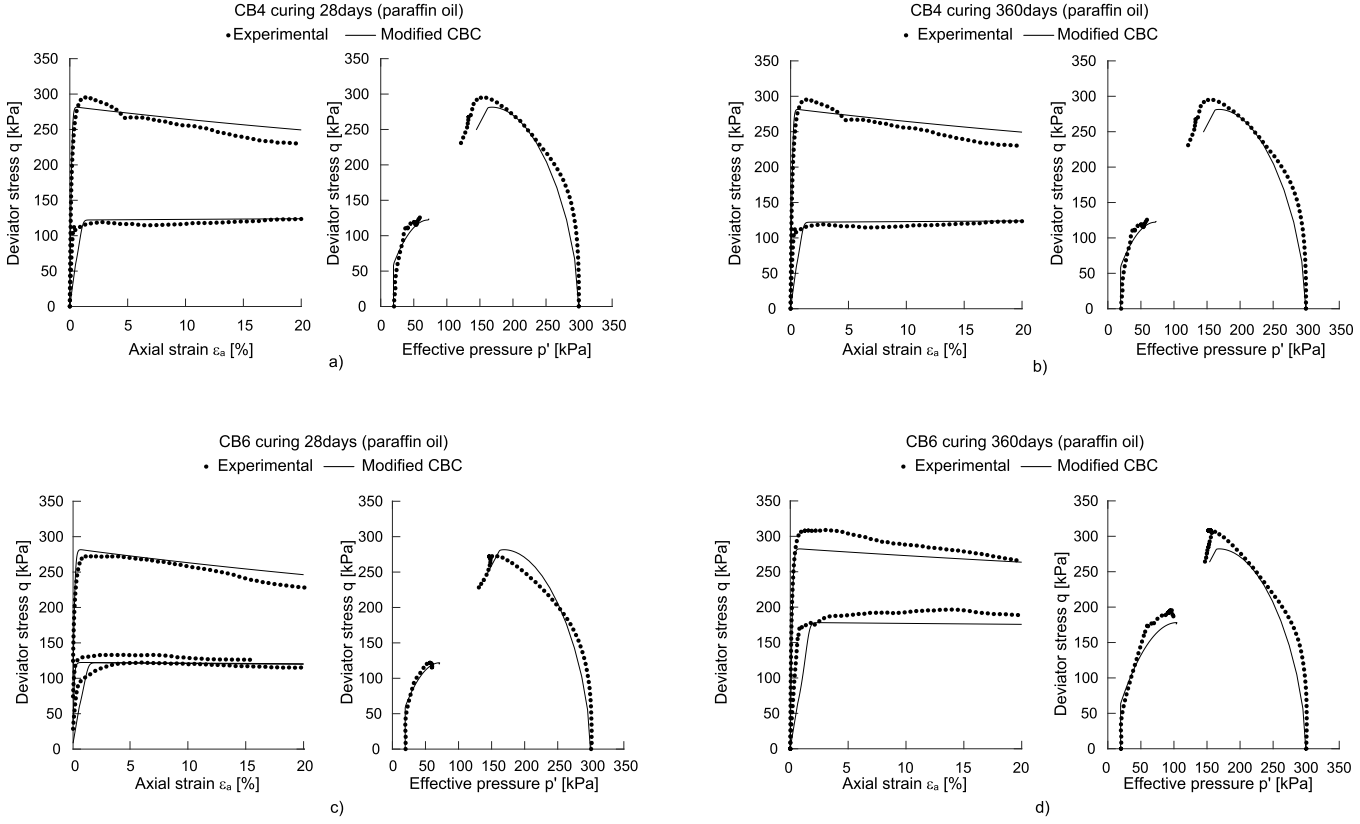

Fig. 17. Comparison between experimental results and model predictions: triaxial tests (curing in paraffin oil).

Table 5
Constitutive model parameters.

Mixture	t[days]	e_0 [–]	ν [–]	κ [–]	λ [–]	M [–]	m [–]	a [–]	p'_{s0} [kPa]	g_1 [–]	h_1 [–]	h_2 [–]	Γ [–]
CB4 (water)	28	9.22	0.25	0.026	1.6	1.7	1.6	0.2	25	0.02	0.15	0.3	16
CB4 (water)	360	10	0.25	0.009	1.35	1.7	1.6	0.2	75	0.02	0.15	0.3	16
CB4 (paraffin oil)	28	8.24	0.25	0.026	1.6	1.7	1.6	0.2	70	0.02	0.32	0.3	14.3
CB4 (paraffin oil)	360	7.85	0.25	0.026	1.5	1.7	1.6	0.2	130	0.02	0.25	0.3	13.5
CB6 (water)	28	6.08	0.25	0.013	1.13	1.7	1.6	0.2	120	0.02	0.32	0.3	10.7
CB6 (water)	360	6.08	0.25	0.008	1.04	1.7	1.6	0.2	210	0.02	0.32	0.3	10.7
CB6 (paraffin oil)	28	6.14	0.25	0.025	1.13	1.7	1.6	0.2	130	0.02	0.32	0.3	10.7
CB6 (paraffin oil)	360	6.08	0.25	0.025	1.04	1.7	1.6	0.2	190	0.02	0.32	0.3	10.7

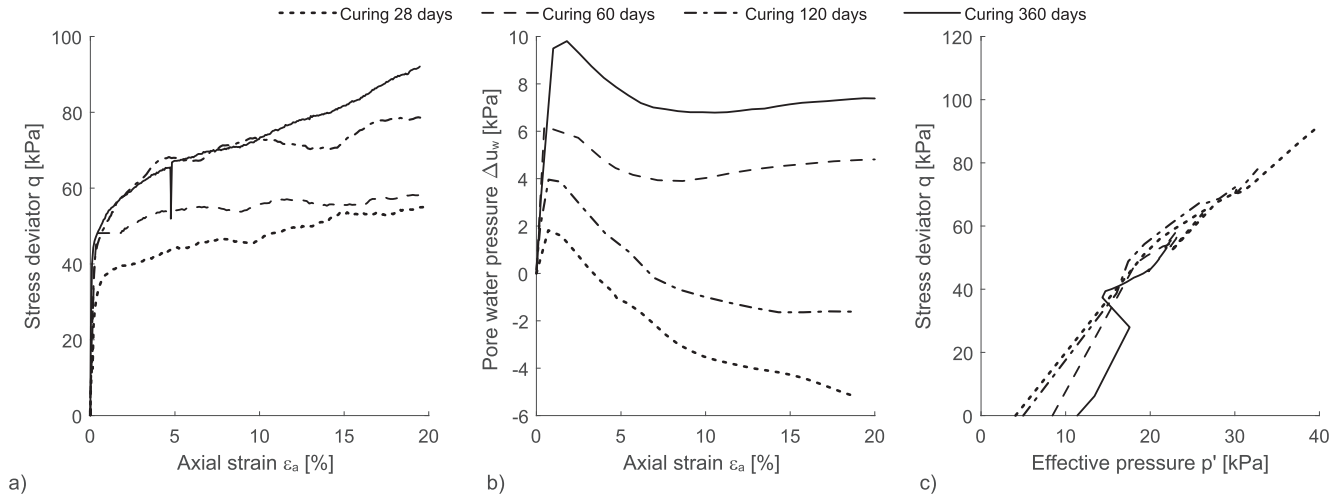

Fig. 18. Mixture CB4 undrained unconsolidated triaxial tests results (curing in water): a) $q-\varepsilon_a$ plane, b) $\Delta u_w-\varepsilon_a$ plane and c) $q-p'$ plane.

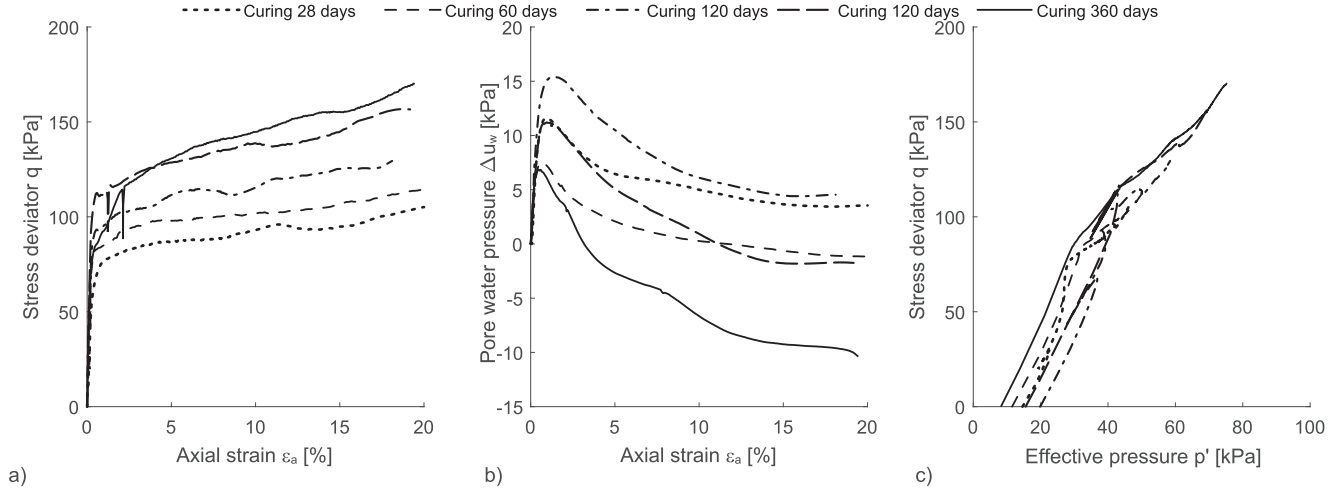

Fig. 19. Mixture CB5 undrained unconsolidated triaxial tests results (curing in water): a) $q-\varepsilon_a$ plane, b) $\Delta u_w-\varepsilon_a$ plane and c) $q-p'$ plane.

Finally, a non-linear elastic law has been adopted, with constant Poisson ratio ν and a bulk stiffness K dependent on p':

$$K = \frac{1+e_0}{\kappa} p' \tag{6}$$

As it can be appreciated in Figs. 14–17, after the parameter calibration (see the procedure discussed in the following section), the modified CBC model allows a very satisfactory reproduction of the experimental results, both along oedometer compression and triaxial shearing paths.

4.1. Parameter calibration

To calibrate the CBC model, the values of ten constitutive parameters, as well as e_0 and the initial value of the hardening variable (p'_{s0})

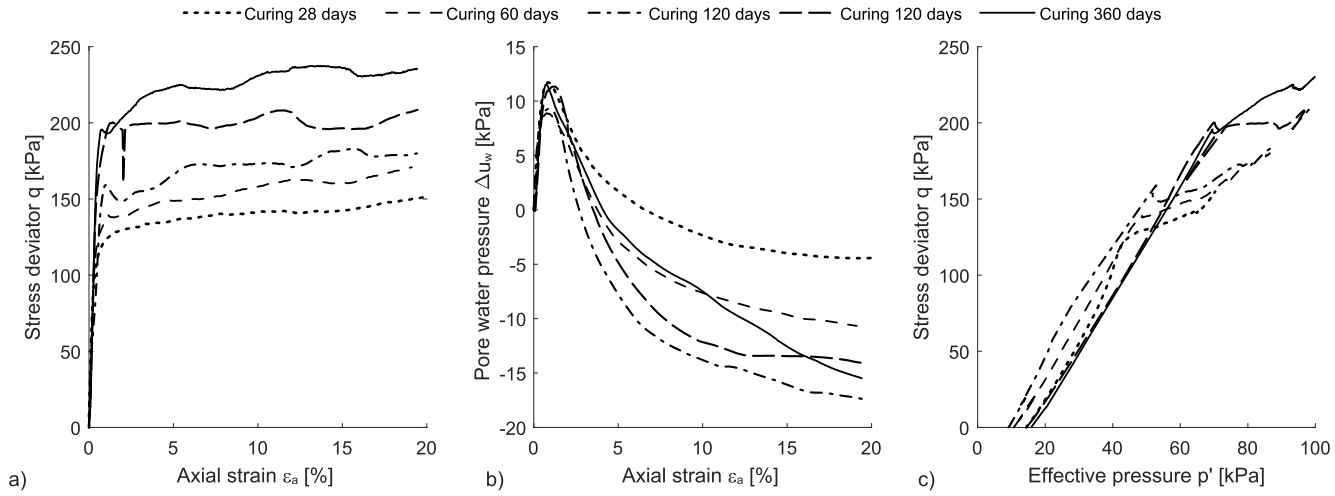

Fig. 20. Mixture CB6 undrained unconsolidated triaxial tests results (curing in water): a) $q-\varepsilon_a$ plane, b) $\Delta u_w-\varepsilon_a$ plane and c) $q-p'$ plane.

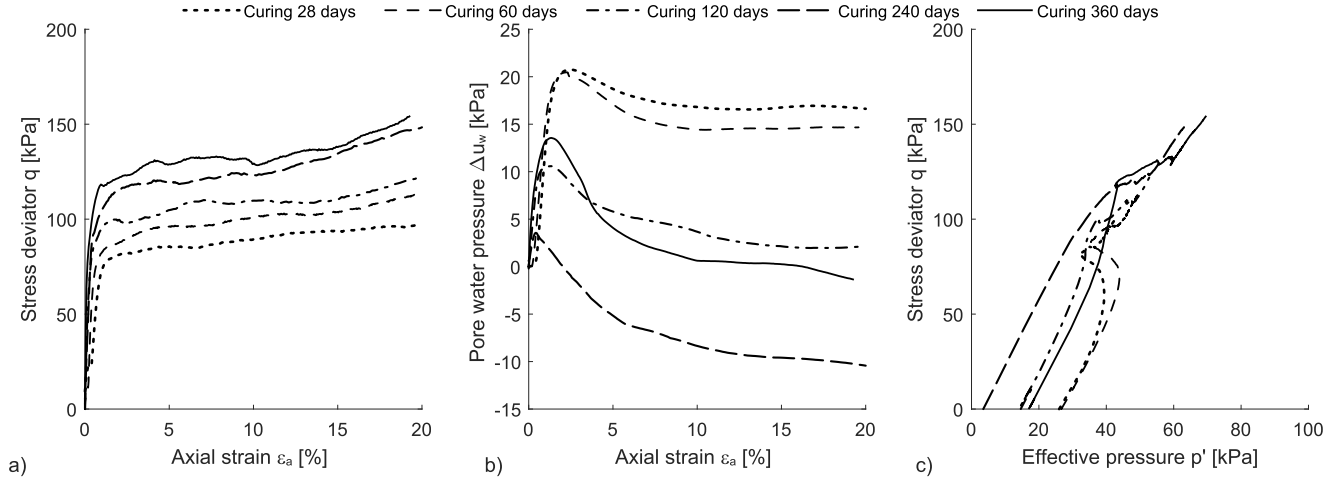

Fig. 21. Mixture CB4 undrained unconsolidated triaxial tests results (curing in paraffin oil): a) $q-\varepsilon_a$ plane, b) $\Delta u_w-\varepsilon_a$ plane and c) $q-p'$ plane.

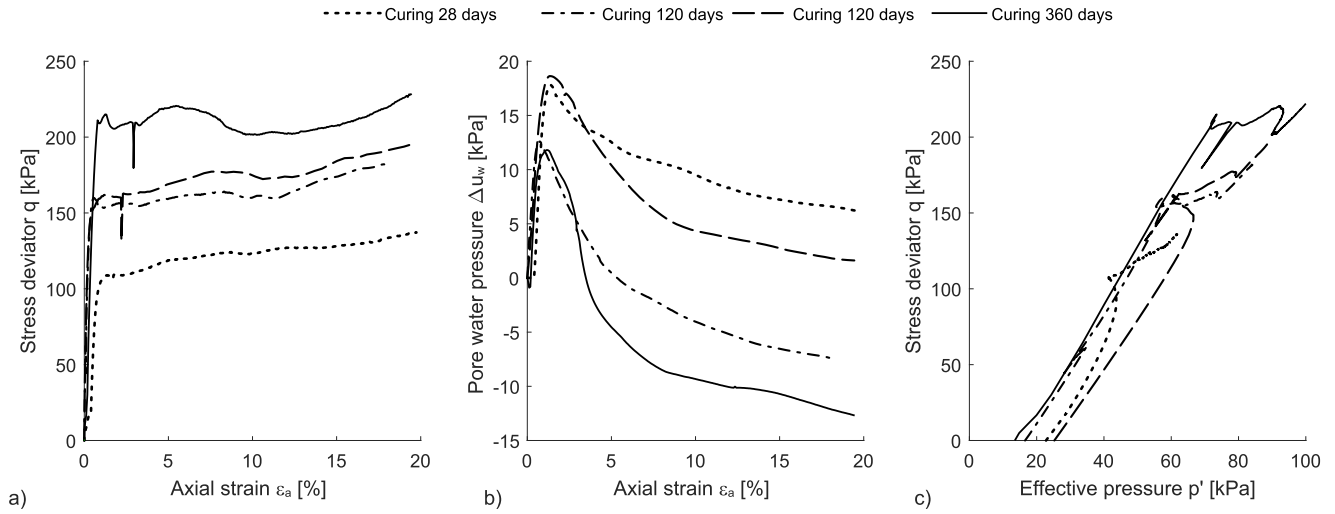

Fig. 22. Mixture CB5 undrained unconsolidated triaxial tests results (curing in paraffin oil): a) $q-\varepsilon_a$ plane, b) $\Delta u_w-\varepsilon_a$ plane and c) $q-p'$ plane.

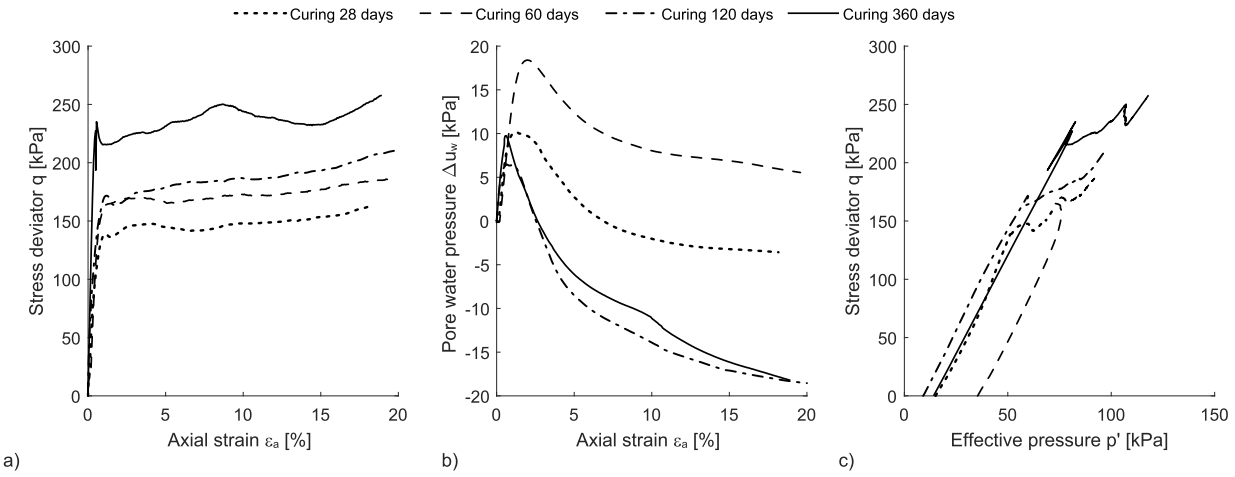

Fig. 23. Mixture CB6 undrained unconsolidated triaxial tests results (curing in paraffin oil): a) $q-\varepsilon_a$ plane, b) $\Delta u_w-\varepsilon_a$ plane and c) $q-p'$ plane.

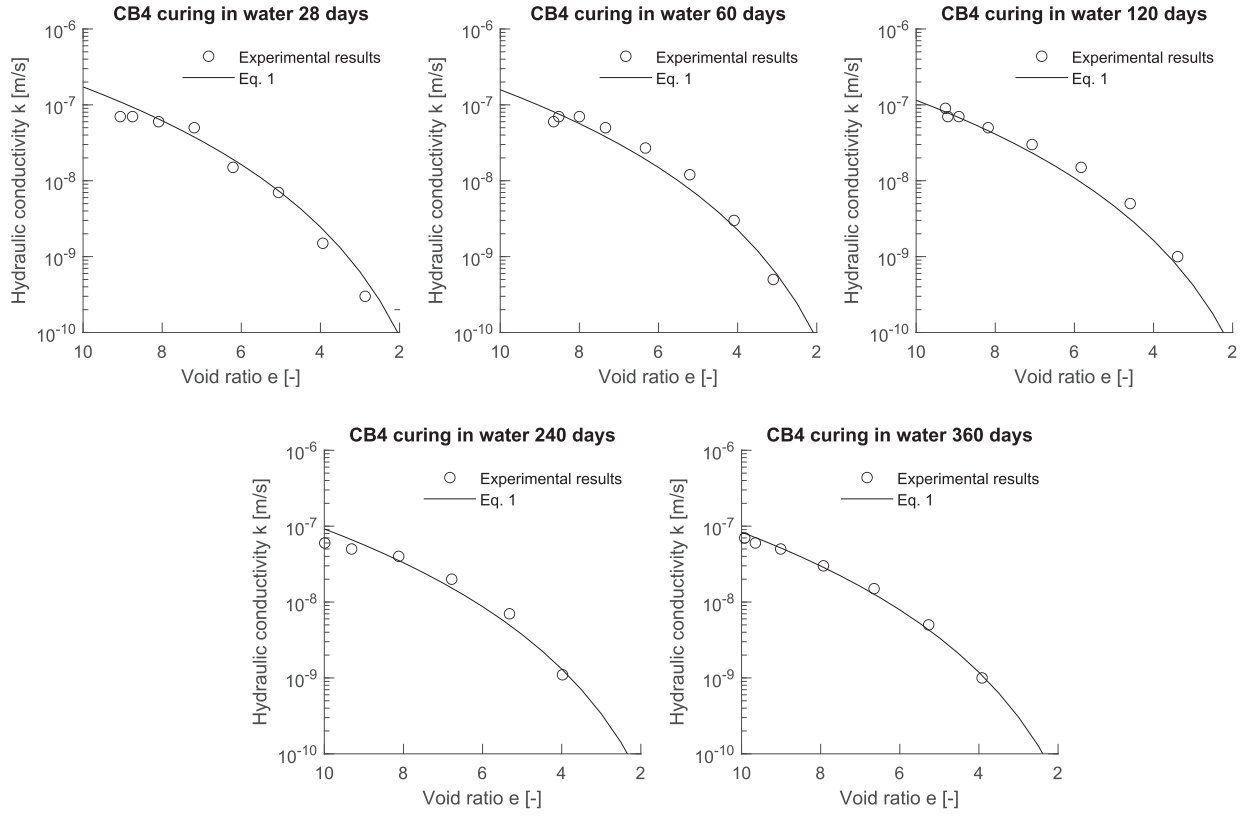

Fig. 24. Mixture CB4 (curing in water) comparison between experimental results and Eq. (1).

have to be defined. e_0 values are calculated from the water content and specific gravity values directly measured after curing. The Poisson ratio ν is assumed to be equal to 0.25, independently on curing time and mixture composition. The CBC model is intended to be an extension of Modified Cam Clay model, therefore λ, κ and p'_{s0} can be calibrated, by following well-established procedures, on oedometer test results. The parameters associated with the shape of the yield function (a, m and M) were calibrated to obtain a yield surface almost coincident with the MMC yield locus on the "wet side" (i.e. for stresses slightly lower than the yield stress), but flatter on the "dry side". As discussed in [12], h_1 can be calibrated independently on the other constitutive parameters on the virgin branch of oedometer test results, whereas g_1 and h_2 are related with the shape of the post peak branch of undrained triaxial test results performed at large confining pressure values. The Γ value can be calibrated on the experimental results to correctly reproduce dilation and compaction obtained when the confining pressure is lower or larger than the yield stress, respectively.

The comparison between experimental oedometer and triaxial test results (points and dotted lines) and model predictions (solid lines) after parameter calibration (their values are reported in Table 5) is reported in Figs. 14–17. For the sake of brevity, the results relative only to two mixtures (CB4 and CB6) are reported. In all the cases considered the proposed constitutive relationship is capable of reproducing both the initial and postpeak response.

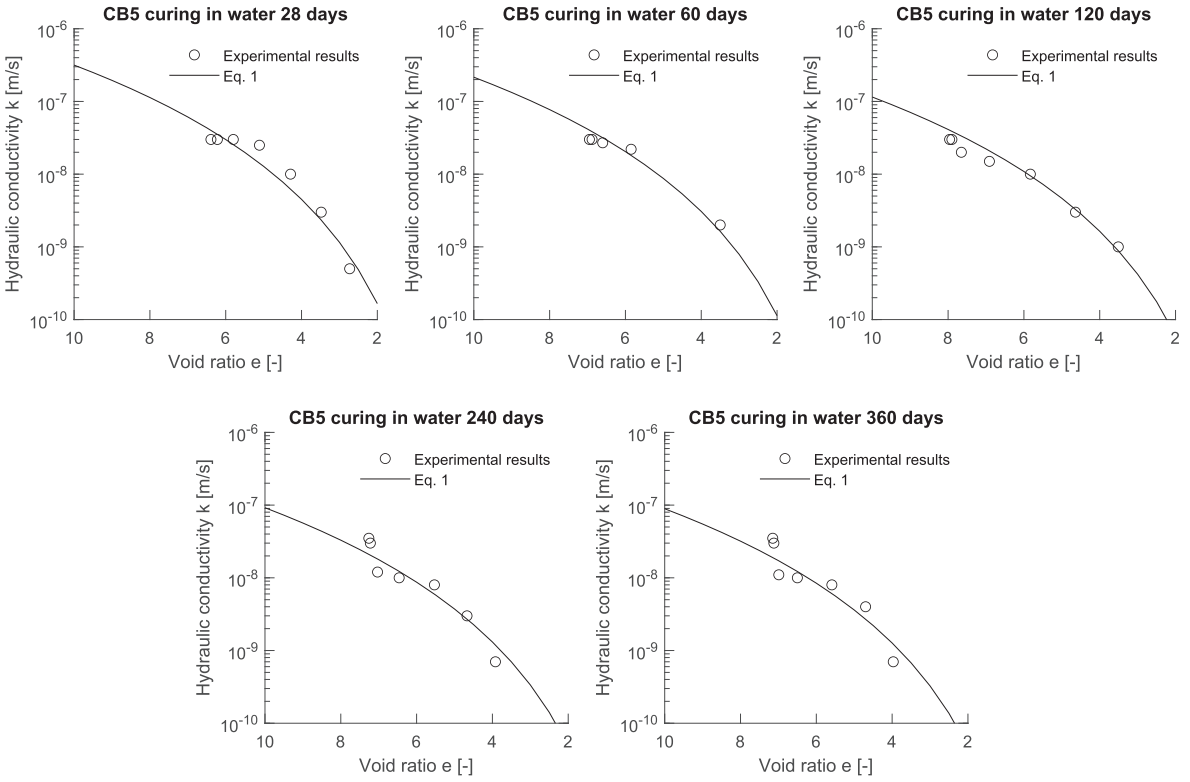

Fig. 25. Mixture CB5 (curing in water) comparison between experimental results and Eq. (1).

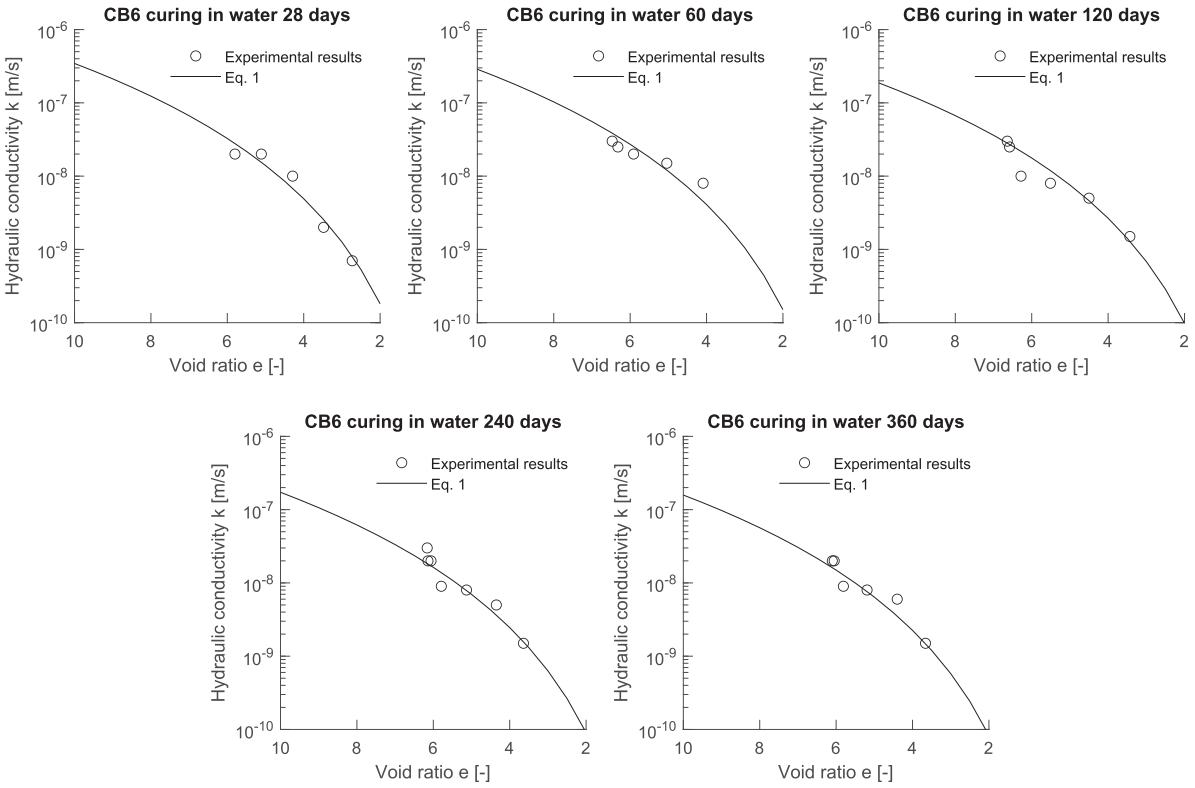

Fig. 26. Mixture CB6 (curing in water) comparison between experimental results and Eq. (1).

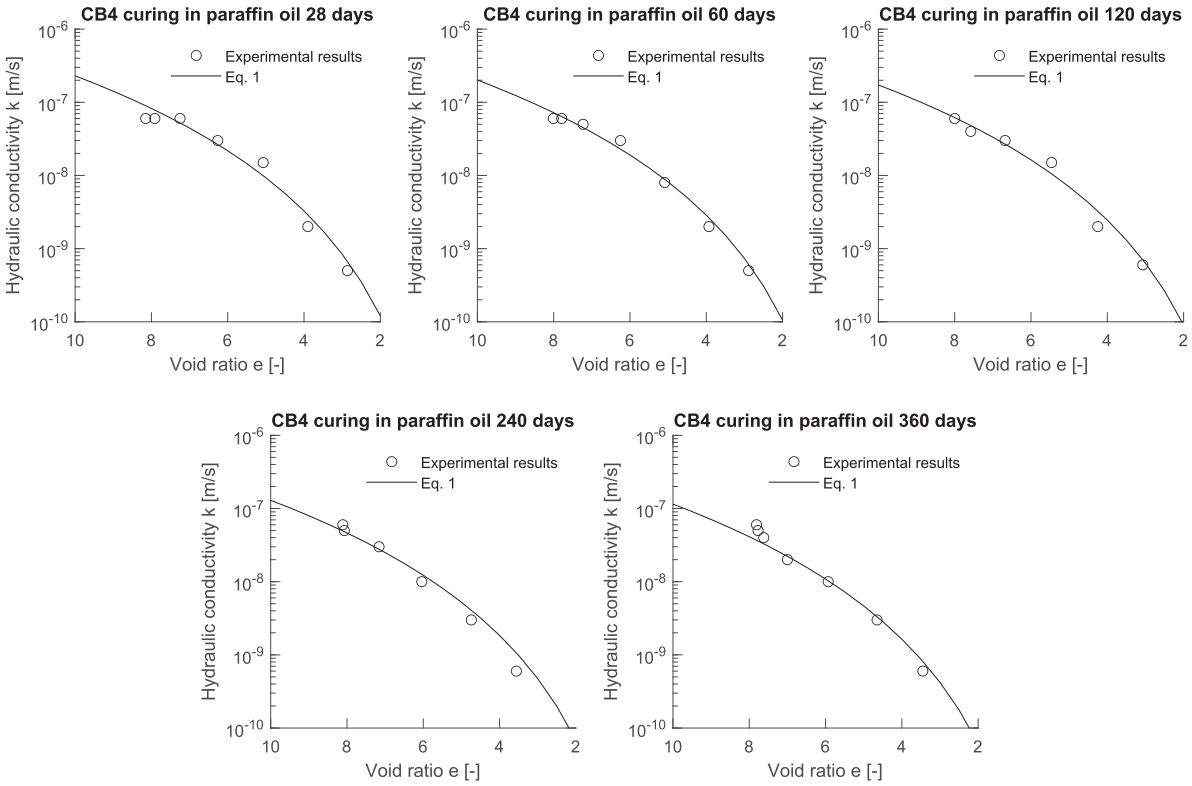

Fig. 27. Mixture CB4 (curing in paraffin oil) comparison between experimental results and Eq. (1).

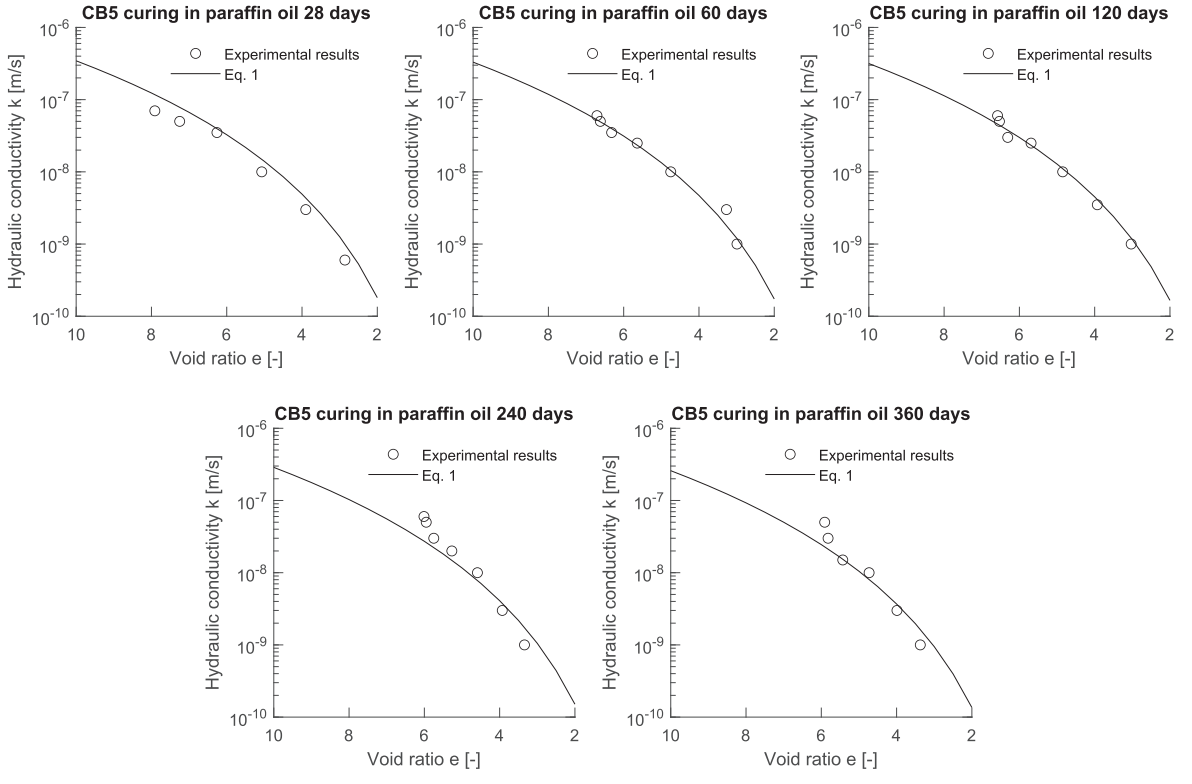

Fig. 28. Mixture CB5 (curing in paraffin oil) comparison between experimental results and Eq. (1).

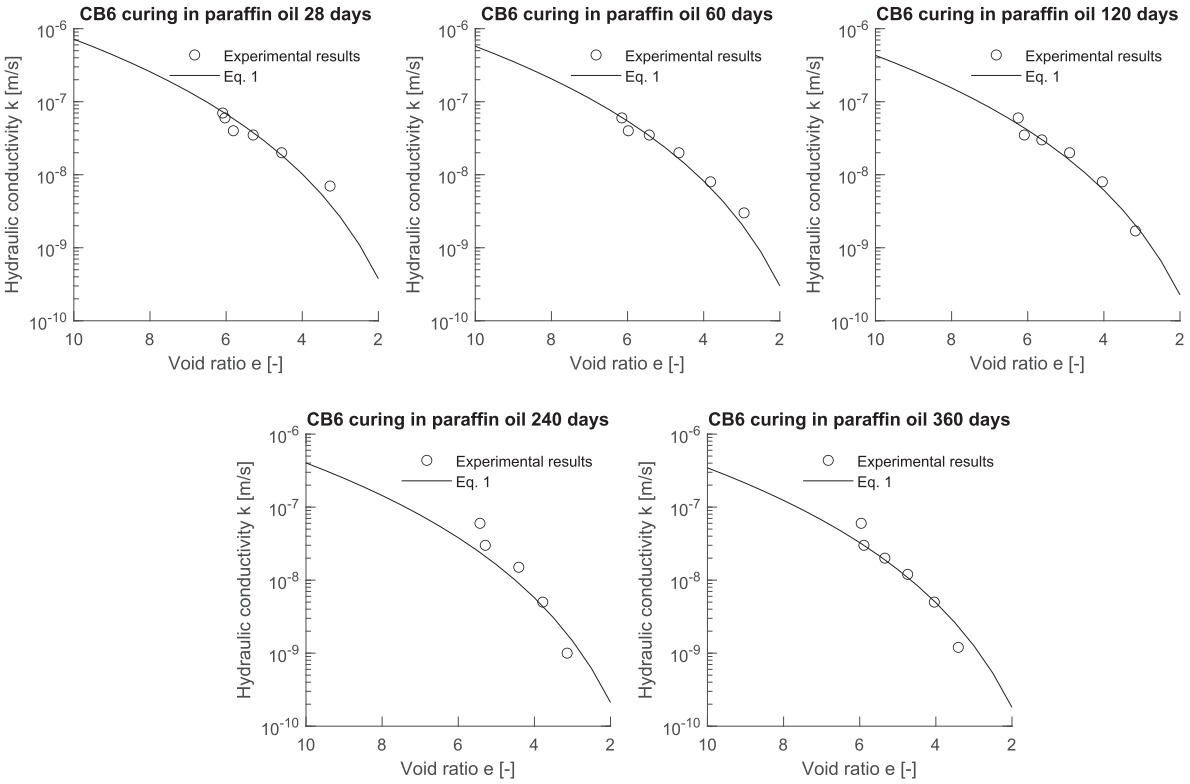

Fig. 29. Mixture CB6 (curing in paraffin oil) comparison between experimental results and Eq. (1).

It is worth noting that curing time only affects λ, κ, e_0 and p'_{s0}, which are parameters that can be easily obtained from standard laboratory tests and procedures.

5. Conclusions

In this paper the experimental results relative to the hydro-mechanical behaviour of cement-bentonite mixtures at different curing times and different curing environments (water and in paraffin oil) are discussed. As was expected for a porous material [25–27,29,30], the hydro-mechanical behaviour is affected by the void ratio (or equivalently by porosity). Moreover, the experimental results clearly show that, by increasing the curing time, both yield pressure and material stiffness increase. The experimental results also highlight that for lower cement contents the hydro-mechanical behaviour is influenced by the curing environment. In fact, larger yield stresses, higher undrained shear strengths, lower void ratios and larger hydraulic conductivity at given void ratios are generally observed in case the samples were cured in paraffin oil. Similar effects are known to occur in bentonites when the ionic concentration of the pore fluid increases. As paraffin oil is non miscible with water, it appears then plausible that the documented differences between the response of the samples cured in water and the one of those cured in paraffin oil are a consequence of different conditions applied with respect to the diffusion of the soluble products of cement hydration and pozzolanic reactions. Diffusion is allowed with water as curing fluid, whereas it is completely inhibited in the case of paraffin oil.

The hydraulic conductivity tends to decrease with curing time and can be estimated, once the void ratio is known, by using a simple Kozeny-Carman like equation, in which the unique parameter depends on cement-bentonite mass ratio and curing conditions. The mechanical behaviour of the material was reproduced by using a stress–strain constitutive relationship (the CBC model) which explicitly accounts for the dependence of the material behaviour on the void ratio [25–27,29,39] and can be calibrated on the results of standard laboratory tests. These tests are necessary to optimize the performance of the cement-bentonite mixture in relation to the site specific conditions. The CBC model was modified by introducing a different yield function more suitable for reproducing the material response at low confining pressures. This represents an important improvement for the model since in shallower portions of cut-off walls cracks are more likely to develop, implying that correctly reproducing the material strength is crucial. From an engineering perspective, the development of strain localizations and cracks in cement-bentonite cut-off walls is particularly critical, since they compromise the barrier effectiveness. Cracks in fact not only modify material strength, but are also preferred pathways for contaminant migration. The constitutive model proposed by the authors can thus be used not only to predict material response along compression paths, but proved also able to correctly reproduce the post-failure response of the material, related to the potential development of cracks.

CRediT authorship contribution statement

Luca Flessati: Conceptualization, Data curation, Formal analysis, Methodology, Software, Validation, Visualization, Writing – original draft, Writing – review & editing. **Gabriele Della Vecchia:** Conceptualization, Methodology, Funding acquisition, Supervision, Writing – review & editing. **Guido Musso:** Conceptualization, Data curation, Methodology, Investigation, Writing – review & editing.

Declaration of Competing Interest

The authors declare that they have no known competing financial interests or personal relationships that could have appeared to influence the work reported in this paper.

Data availability

Some or all data, models, or code that support the findings of this study are available from the corresponding author upon reasonable request.

Acknowledgements

The previous activity of the first author was financed in the context of the public administration agreement between Politecnico di Milano – Department of Civil and Environmental Engineering and the Italian Ministry of Economic Development, Direzione Generale per la Sicurezza anche Ambientale delle Attività Minerarie ed Energetiche–Ufficio Nazionale Minerario per gli Idrocarburi e le Georisorse–Programme Clypea, which is here gratefully acknowledged.

A. Appendix Unconsolidated undrained triaxial test results

The results relative to unconsolidated undrained triaxial tests are reported in Figs. 18–23. In particular, the results relative to curing in water are reported in Figs. 18–20 (mixtures CB4, CB5 and CB6, respectively), whereas the ones to curing in paraffin oil in Figs. 21–23 (mixtures CB4, CB5 and CB6, respectively).

Appendix B. Calibration of Kozeny-Carman law

In Figs. 24–29 the comparison between experimental data and the predictions with Kozeny-Carman law are reported. In particular, Figs. 24–26 are relative to curing in water (mixtures CB4, CB5 and CB6, respectively), whereas Figs. 27–29 to curing in paraffin oil (mixtures CB4, CB5 and CB6, respectively).

References

[1] J.H. Deschenes, M. Massiera, J.P. Tournier, Testing of a cement-bentonite mix for a low-permeability plastic barrier, ASTM Special Technical Publication 1293 (1995) 252–270.
[2] S.M. Opdyke, J.C. Evans, Slag-cement-bentonite slurry walls, J. Geotech. Geoenviron. Eng. 131 (6) (2005) 673–681.
[3] K. Joshi, C. Kechavarzi, K. Sutherland, M.Y.A. Ng, K. Soga, P. Tedd, Laboratory and in situ tests for long-term hydraulic conductivity of a cement-bentonite cutoff wall, J. Geotech. Geoenviron. Eng. 136 (4) (2010) 562–572.
[4] M. Williams, G.S. Ghataora, Effect of fibre reinforcement on the properties of ground granulated blast furnace slagcement–bentonite slurry, Studia Geotechnica et Mechanica 33 (4) (2011) 63–83.
[5] S. Jefferis, Cement-bentonite slurry systems, Grouting and Deep Mixing 2012 (2012) 1–24.
[6] A. Royal, Y. Makhover, S. Moshirian, D. Hesami, Investigation of cement–bentonite slurry samples containing pfa in the ucs and triaxial apparatus, Geotech. Geol. Eng. 31 (2) (2013) 767–781.
[7] K. Soga, K. Joshi, J. Evans, Cement bentonite cutoff walls for polluted sites, in: Proceedings of the 1st international symposium on Coupled Phenomena in Geotechnical Engineering, Manassero et al. (Eds), Taylor & Francis Group, London, 2013, 149–165.
[8] A. Royal, A. Opukumo, C. Qadr, L. Perkins, M. Walenna, Deformation and compression behaviour of a cement–bentonite slurry for groundwater control applications, Geotech. Geol. Eng. 36 (2) (2018) 835–853.
[9] G. Guida, G. Musso, G. Sanetti, C. di Prisco, G. Della Vecchia, A procedure to estimate cutoff wall transport properties from monitoring wells, Int. J. Numer. Anal. Methods 45 (9) (2021) 1282–1299.
[10] G. Musso, V. Vespo, G. Guida, G. Della Vecchia, Hydro-mechanical behaviour of a cement–bentonite mixture along evaporation and water-uptake controlled paths, Geomech. Energy Environ. 100413 (2022), https://doi.org/10.1016/j.gete.2022.100413.
[11] J.M.R. Carreto, L.M.M.S. Caldeira, E.J.L.M.D. Neves, Hydromechanical characterization of cement-bentonite slurries in the context of cutoff wall applications, J. Mater. Civ. Eng. 28 (2) (2016) 04015093.
[12] L. Flessati, G. Della Vecchia, G. Musso, Mechanical behavior and constitutive modeling of cement–bentonite mixtures for cutoff walls, J. Mater. Civ. Eng. 33 (3) (2021) 04020483.
[13] E. Fratalocchi, E. Pasqualini, P. Balboni, Performance of a cement-bentonite cut-off wall in an acidic sulphate environment, in: 5th ICEG Environmental Geotechnics: Opportunities, Challenges and Responsibilities for Environmental Geotechnics: Proceedings of the ISSMGE's fifth international congress organized by the Geoenvironmental Research Centre, Cardiff University and held at Cardiff City Hall on 26–30th June 2006 (pp. 133-139). Thomas Telford Publishing, 2006.
[14] E. Fratalocchi, V. Brianzoni, F. Mazzieri, E. Pasqualini, Durability of cement-bentonite cut-off walls in sulphate solutions, in: Geo-Chicago 2016, 2016, pp. 695–704.
[15] A. Akbarpour, M. Mahdikhani, Effects of natural zeolite and sulfate environment on mechanical properties and permeability of cement–bentonite cutoff wall, European Journal of Environmental and Civil Engineering, 1-14. [13] Lancellotta, R. (2008). Geotechnical engineering. CRC Press, 2022.
[16] C. Chao, C. Jommi, S. Muraro, Numerical investigation of the equipment set-up in triaxial testing of soft soils, in: Proceedings 10th NUMGE 2023 10th European Conference on Numerical Methods in Geotechnical Engineering Zdravković L, Konte S, Taborda DMG, Tsiampousi A (eds), 2023.
[17] E. Romero, A microstructural insight into compacted clayey soils and their hydraulic properties, Eng. Geol. 165 (2013) 3–19.
[18] A. Azizi, G. Musso, C. Jommi, Effects of repeated hydraulic loads on microstructure and hydraulic behaviour of a compacted clayey silt, Can. Geotech. J. 57 (1) (2020) 100–114.
[19] J.K. Mitchell, K. Soga, Fundamentals of soil behavior (Vol. 3, p. USA), John Wiley & Sons, New York, 2005.
[20] D. Plee, F. Lebedenko, F. Obrecht, M. Letellier, H. Van Damme, Microstructure, permeability and rheology of bentonite—cement slurries, Cem. Concr. Res. 20 (1) (1990) 45–61.
[21] C. Di Maio, Exposure of bentonite to salt solution: osmotic and mechanical effects, Géotechnique 46 (4) (1996) 695–707.
[22] E. Castellanos, M.V. Villar, E. Romero, A. Lloret, A. Gens, Chemical impact on the hydro-mechanical behavior of high-density FEBEX bentonite, Phys. Chem. Earth 33 (2008) S516–S526.
[23] G. Della Vecchia, G. Musso, Some remarks on single-and double-porosity modeling of coupled chemo-hydro-mechanical processes in clays, Soils Found. 56 (5) (2016) 779–789.
[24] B. Loret, T. Hueckel, A. Gajo, Chemo-mechanical coupling in saturated porous media: elastic–plastic behaviour of homoionic expansive clays, Int. J. Solids Struct. 39 (10) (2002) 2773–2806.
[25] G. Musso, A. Azizi, C. Jommi, A microstructure-based elastoplastic model to describe the behaviour of a compacted clayey silt in isotropic and triaxial compression, Can. Geotech. J. 57 (7) (2020) 1025–1043.
[26] K. Been, M.G. Jefferies, A state parameter for sands, Géotechnique 35 (2) (1985) 99–112.
[27] X.S. Li, Y.F. Dafalias, Dilatancy for cohesionless soils, Geotechnique 50 (4) (2000) 449–460.
[28] R. Lagioia, A. Puzrin, D. Potts, A new versatile expression for yield and plastic potential surfaces, Comput. Geotech. 19 (3) (1996) 171–191.
[29] V. Revilla-Cuesta, F. Faleschini, M.A. Zanini, M. Skaf, V. Ortega-López, Porosity-based models for estimating the mechanical properties of self-compacting concrete with coarse and fine recycled concrete aggregate, J. Build. Eng. 44 (2021) 103425.
[30] B. Cantero, I.F. Sáez del Bosque, A. Matías, M.I. Sánchez de Rojas, C. Medina, Water transport mechanisms in concretes bearing mixed recycled aggregates, Cem. Concr. Compos. 107 (2020) 103486.